Available online at www.sciencedirect.com

SCIENCE DIRECT®

Marine Micropaleontology 56 (2005) 50–79

MARINE MICROPALEONTOLOGY

www.elsevier.com/locate/marmicro

Surface water dynamics and phytoplankton communities during deposition of cyclic late Messinian sapropel sequences in the western Mediterranean

José-Abel Flores[a,*], Francisco J. Sierro[a], Gabriel M. Filippelli[b], María Ángeles Bárcena[a], Marta Pérez-Folgado[a], Antonio Vázquez[c], Rosa Utrilla[c]

[a]*Departamento de Geología, Universidad de Salamanca, 37008 Salamanca, Spain*
[b]*Department of Geology, Indiana University-Purdue University Indianapolis, USA*
[c]*Institute of Earth Sciences "Jaume Almera", CSIC, Solé Sabarís s/n, 08028 Barcelona, Spain*

Received 18 October 2004; received in revised form 16 March 2005; accepted 14 April 2005

Abstract

Distinctive precession-scale sapropel/marl sequences of late Messinian age are found in several outcrops bordering the western Mediterranean. To examine the roles of stratification and productivity in driving this cyclic sedimentation, we performed a high resolution analysis of calcareous nannofossil assemblages through four orbital sequences (composed of sapropel/marl/diatomite/marl) from the Sorbas basin in southern Spain. This effort also involved a detailed comparison between calcareous nannofossil abundances and other micropaleontological, sedimentological and geochemical proxies to further understand the behaviour of some taxa. For this period, fluctuations in the depth and gradient of the pycnocline, and the distribution and remobilization of nutrients seem to be the main factors controlling the calcareous nannoplankton assemblages, with temperature of secondary importance.

In the sapropels, the warm-oligotrophic genus *Sphenolithus* and *Discoaster* are abundant. Especially significant is the progressive increase towards the top of *Discoaster pentaradiatus*, indicator of severe oligotrophic (deep pycnocline) conditions. At the top of the sapropels, peaks in *Reticulofenestra rotaria* are interpreted here as the result of an increase of surface water temperatures, although decreasing salinity may also play a role. Small *Reticulofenestra* (<5 μm) is the major component of the overlying marl, and peaks in episodes of high nutrient availability (assessed here by the phosphorus proxy P/Ti). This morphotype is linked to a relatively shallow deep chlorophyll maximum, with a stable but shallow thermocline. Overlying the marl is a diatomite bed, interpreted here as an indicator of peak nutrient availability (confirmed by P/Ti ratios), with a reduction of calcareous nannofossils due to nutrient competition and dilution. Interestingly, however, species such as *Reticulofenestra pseudoumbilicus* (>5 μm) are more frequent in diatomites even considering conditions of extreme mixing and eutrophication occurred in the basin. *Umbilicosphaera jafari* peaks just after diatomites, replacing small *Reticulofenestra*, probably as a response to an increase in salinity and/or nutrient limitation. Species such as *Coccolithus pelagicus* and

* Corresponding author. Tel.: +34 923 294497; fax: +34 923 294514.
E-mail address: flores@usal.es (J.-A. Flores).

0377-8398/$ - see front matter
doi:10.1016/j.marmicro.2005.04.002

Helicosphaera carteri are abundant at the top of the diatomites and in the overlying marls, indicating relatively mesotrophic and cool water conditions.

This succession shows similar characteristics in the four studied cycles, allowing us to interpret surface water dynamics in this region on orbital time scales. The top of the sapropel represents a warm, low salinity and well stratified episode under a situation of maximum insolation. A well developed pycnocline and oligotrophic conditions (moderate production of calcareous phytoplankton) coinciding with anoxic conditions at the bottom enhance the preservation of organic matter, and consequently generate a sapropel. Diatomites are deposited under a situation of unstable pycnocline that produce an increase in productivity in surface waters. Diatoms significantly deplete limiting nutrients, and consequently calcareous nannofossils start to be dominant again in the water column as result of a progressive stabilization of the pycnocline.

Keywords: Messinian; Miocene; Neogene; Sapropels; Mediterranean; Paleoceanography; Paleoecology; Calcareous nannofossils; Planktonic foraminifers; Biochemical cycles

1. Introduction

The widespread deposition of sapropels, often with marl interbeds, in the Mediterranean during the Miocene to Holocene has been studied by different authors using sedimentological, micropaleontological and geochemical techniques (Kidd et al., 1978; Hilgen, 1991; Comas et al., 1996; Emeis et al., 1996; Cramp and O'Sullivan, 1999; Rohling, 1994; Sierro et al., 2001, among others). Most of these studies argue that these sequences are linked to climatic or oceanographic variations (with some modification by tectonic or diagenetic processes), with more recent high resolution work further indicating that the sapropel/marl sequences are related to precession-scale orbital variations.

A beautiful representation of the Miocene sequence outcrops in the Sorbas Basin (Fig. 1), located in the western Mediterranean. Here, these alternating sapropel/marl sequences with diatomite layers (Fig. 2) appear after 6.7 Ma (Sierro et al., 2001, 2003). The sapropels were likely deposited under conditions of minimum precession (maximum summer insolation), reflected by an increase in precipitation and runoff in the Mediterranean basin, which drove an increased stratification of surface waters. The marls were deposited during the subsequent increase of the precession

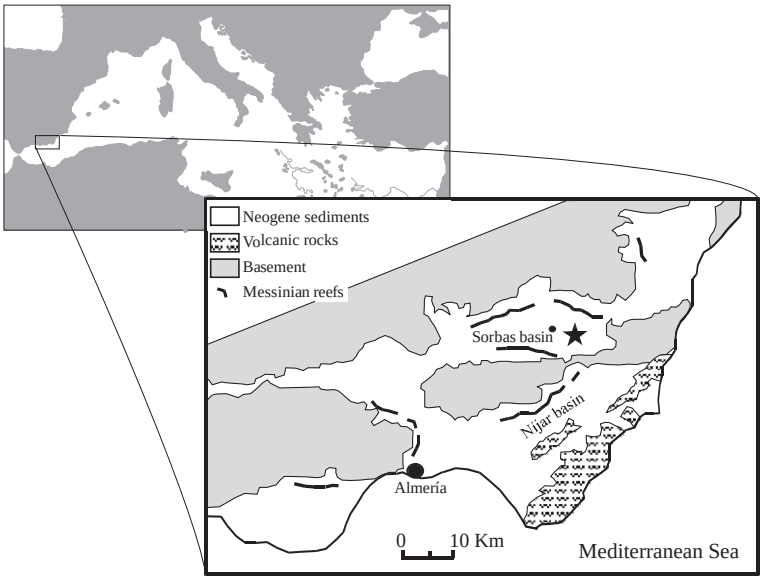

Fig. 1. Location of the Sorbas basin in south-eastern Spain. Star marks the studied outcrop.

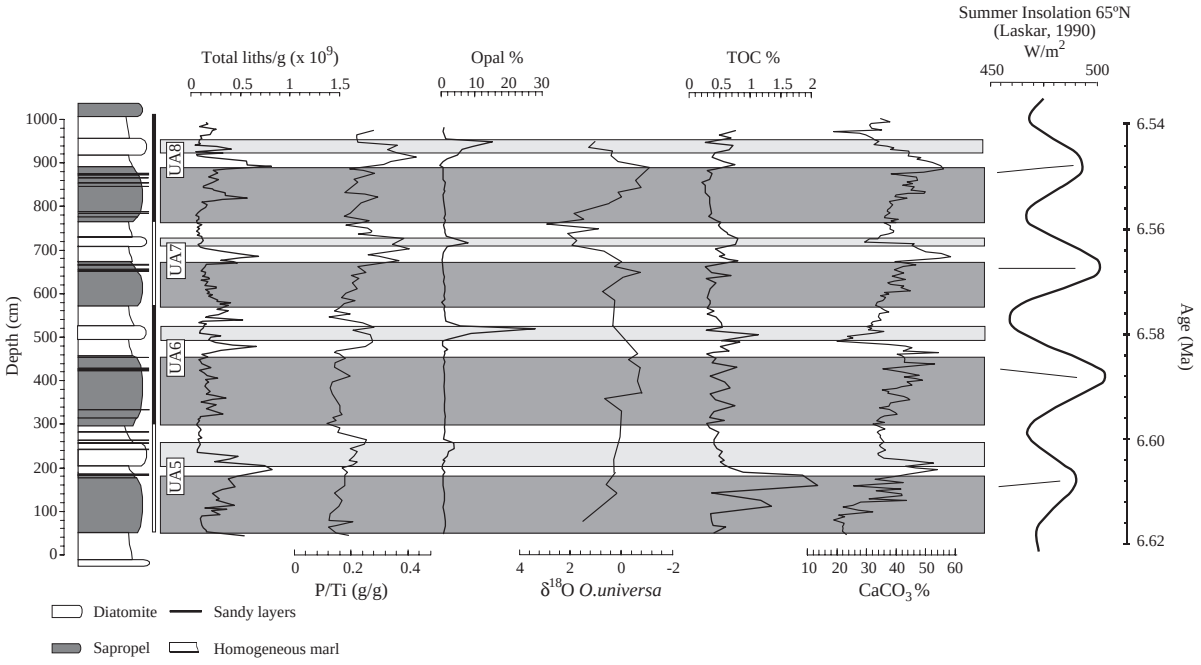

Fig. 2. Stratigraphic column of four cycles from the Los Molinos section of the Upper Abad Member (UA) in the Sorbas basin. Total abundance of calcareous nannofossils (liths per g), Phosphorus–Titanium ratio (after Filippelli et al., 2003) and percentages of opal, total organic matter (TOC) and calcium carbonate (Appendix B and Appendix C). Dark grey bands are sapropels, light grey bands are diatomites, white bands are marls. Summer insolation curve after Laskar (1990) based on the Sierro et al. (2001) interpretation (and calibration) correlating top of sapropels with maxim in insolation.

index (reduction of summer insolation), reflected by a dry and cold climate and an increase in evaporation, resulting in the mixing and reoxygenation of deep and bottom waters and reduced preservation of organic matter (Rossignol-Strick, 1985; Hilgen, 1991; Sierro et al., 1999), explaining the low record of total organic matter (TOC) observed in our record (Fig. 2). This pattern is not identical in all of the Mediterranean during the Miocene; in the eastern Mediterranean basin, sapropels are replaced by diatomites (Hilgen et al., 1995; Sprovieri et al., 1996; Krijgsman et al., 1995; Schenau et al., 1999; Pérez-Folgado et al., 2003).

Calcareous nannofossils are an important component of these sediments (Muller, 1985; De Kaenel and Villa, 1996; Castradori, 1998; Negri et al., 1999a,b; Negri and Villa, 2000; Vázquez et al., 2000); they have been used mainly for biostratigraphy and occasionally in paleoceanographic reconstruction. As directly related to Coccolithophores, most calcareous nannoplankton were a significant component of the phytoplankton inhabitant at different levels of the photic zone. For the late Miocene, most of the recorded species are extinct, and thus interpretations of their behaviour and environmental conditions are not well-constrained (e.g. Young, 1994). One of the goals of this study is to analyze the calcareous nannofossil assemblages and their relationship with lithology, geochemical proxies related to nutrient conditions, and other micropaleontological groups (i.e. foraminifers and diatoms). Our ultimate aim is to more accurately reconstruct oceanographic dynamics in the Mediterranean at the end of the Miocene, just before the *Salinity Crisis* (Hsü et al., 1973; Van Couvering et al., 1976).

2. Materials and methods

2.1. Location of the studied section and materials

The Abad Member (Völk and Rondeel, 1964; Ott d'Estevou, 1980; Montenat and Ott d'Estevou,

1996;) was deposited in the Sorbas basin (SE Spain) (Fig. 1) during the late Miocene (pre-evaporite Messinian) in a tectonically active marginal basin. The Upper Abad member (UA) consists of a total of 34 cycles alternating sapropels and homogeneous marls. The bathymetry estimated ranges from deeps of 1100 m for the first cycles (Krijgsman et al., submitted for publication) to ca. 150 m water depth for the latest (Troesltra et al., 1980). Here we studied four of the first Upper Abad cycles: UA5 to UA8.

Sedimentary cycles in Sorbas are quadripartite and consist of a sapropel at the base, followed by a lower homogeneous marl, a diatomite and an upper homogeneous marl at the top of the cycle (Fig. 2). The sapropels in Sorbas, following the terminology of Hilgen et al. (1995) are very thick (~1 m) and consist of brownish laminated marls. Thin beds (~10 cm) of black-grey clays are frequent in all sapropels. Lamination is especially well developed in the middle part of the sapropels, whereas it is weakly developed in the upper and lower parts where bioturbation is slightly more intense. The homogeneous strata are soft green marls ranging in thickness from 25 to 45 cm. The diatomites are white, sometimes weakly laminated deposits of around 20 cm in thickness. As it is possible to observe in Fig. 2, the total organic matter (TOC) does not increase its percentage in sapropels. These sediments are the result of low organic production and good organic preservation during sapropels alternating with high organic production and intense oxygenation with the consequent reduction in TOC during diatomite deposition (Hilgen, 1991; Sierro et al., 1999; Sierro et al., 2003; Filippelli et al., 2003).

2.2. Chronology

The late Mediterranean rhythmic cyclostratigraphic patterns have been intensively studied over the past years (Sierro et al., 1999; Krijgsman et al., 1999; Vázquez et al., 2000) and the Abad composite, based on several sections from the Sorbas basin, was proposed as a standard reference section for the late Messinian part of the Astronomical Polarity Time Scale (Sierro et al., 2001).

The sequence of sapropelitic beds interbedded within homogeneous marls represents the most common response to orbitally driven climatic variability and has been used to construct astronomical time scales (Hilgen, 1991; Hilgen et al., 1995; Hilgen and Krijgsman, 1999; Krijgsman et al., 1999, 2001). Variation in precipitation, runoff and wind intensity is responsible for changes in deposition conditions and in lithology. These alternating conditions are also observed in variations in the planktonic and benthic foraminifer assemblages (Sierro et al., 2003; Pérez-Folgado et al., 2003). Krijgsman et al. (1999) and Sierro et al. (2001) astronomically calibrated the Abad member layers, and tuned the 65° N summer insolation record after Laskar (1990). Every defined cycle represents a precessional interval. The selected interval ranges from 6.62 to 6.54 Mys; that represents about 80 Kys (Fig. 2).

2.3. Techniques

For the study of calcareous nannofossils a total of 174 samples were analyzed using a polarizing light and scanning electron microscope from 4 cycles representing a resolution of less than 0.4 Kys. Samples were prepared following the Flores and Sierro (1997) technique. A total of at least 300 liths larger than 3 μm were counted in random fields of view. Additionally, in the same number of fields of view liths smaller than 3 μm are independently counted. For species with low abundances we extended the counting to at least 25 random fields of view. Results are presented in absolute (liths per gram) for the total assemblage and in relative (percentages) abundances for the identified taxa (Appendix B). In addition, routine Scanning Electron Microscope (SEM) analyses were performed in selected samples to evaluate the preservation of calcareous nannofossils. Liths in the samples studied show preservation from moderate to good. Small liths and other easily dissolved species are always present in the samples. Occasional overgrowths are present on some asteroliths, but this feature never prevents their identification at species level. The slides analyzed are deposited in the Micropaleontological Collections at the University of Salamanca.

For the same material, although with different time resolution, data concerning foraminifers and diatoms were raised by Pérez-Folgado et al. (2003). Geochemical data sets are from Filippelli et al. (2003). For this study, the P/Ti ratio of bulk sediments is used—this proxy provides a reference for

net excess P deposition (beyond the terrigenous contribution). As P is a biolimiting nutrient (Filippelli, 2001), the P/Ti ratio can be used as a measure of total biological productivity. Other data such as opal, calcium carbonate and TOC, as well as techniques used for their determination, are in Vázquez et al. (2000), although for this study sampling resolution was improved (Appendix C).

3. Results

Figs. 3–6 show the relative abundance of different calcareous nannofossil taxa along the studied cycles. With few exceptions, a similar pattern is observed in every cycle, indicating a repetitive response to changes in environmental conditions. Maximum values in total calcareous nannofossils occur at lower marls, minima during the diatomite and upper marls, and moderate abundances in sapropels. The total nannofossil shows a parallel record with calcium carbonate, mainly due to pelagic rain (planktonic foraminifers and calcareous nannoplankton) (Vázquez et al., 2000). One exception is observed in sapropel UA8, where a peak is observed in the middle portion (due to an increase in *Reticulofenestra* <5 μm) coinciding with a similar feature in the P/Ti record (Fig. 2).

Reticulofenestra <5 μm is the most abundant morphotype following a regular pattern with relatively high percentages in the upper part of sapropels and in the lower marls, and a drastic reduction from the base of diatomites and in the upper marls. An exception is diatomite UA8 where the percentage of *Reticulofenestra* <5 μm is high. On the other hand, *Reticulofenestra pseudoumbilicus* (>5 μm) is particularly abundant in diatomites. Other Reticulofenestrids, such as *Reticulofenestra rotaria* occur in low proportions, but showing significant peaks in the upper part of sapropels (Fig. 3).

Discoaster sl. (total) is more abundant in the upper half of sapropels and in the lower marls. A peak is also observed at top of UA8. This general trend in *Discoaster* is mainly due to *Discoaster variabilis*, the most abundant species; however, it is important to note that, with some exceptions, *Discoaster pentaradiatus* and *Discoaster brouweri* occur at the top of sapropels or in the lower marls, reaching values close to 2% of total assemblage (Fig. 4).

Sphenolithus abies and *Spenolithus neoabies* (here considered together) are more abundant in sapropels

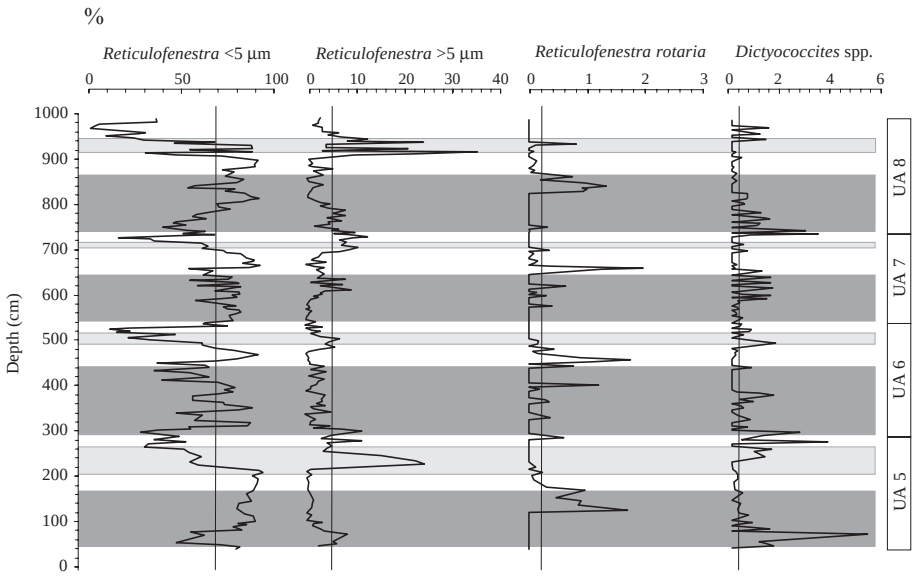

Fig. 3. Relative abundances (percentage) of reticulofenestrids identified in the four analyzed cycles (Appendix B). The thin line crossing plots represents the media. Dark grey bands are sapropels, light grey bands are diatomites, white bands are marls.

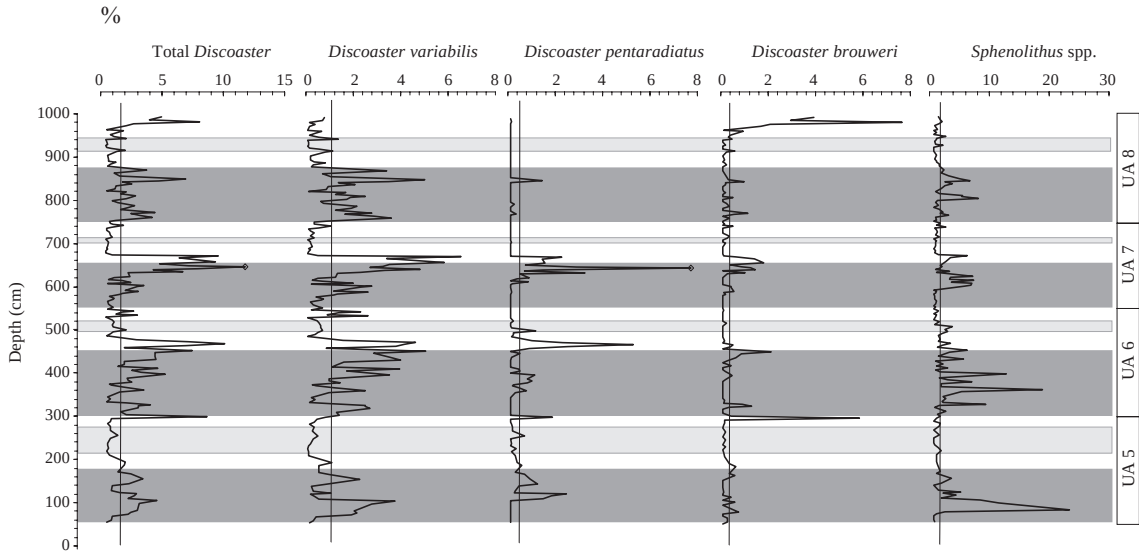

Fig. 4. Relative abundances (percentage) of asteroliths and sphenoliths identified in the four analyzed cycles (Appendix B). The thin line crossing plots represents the media. Dark grey bands are sapropels, light grey bands are diatomites, white bands are marls.

and reduce progressively their abundance towards the upper marls, where reach the lower values. In the diatomite of UA6, *Sphenolithus* show a small, but noteworthy peak (Fig. 4).

Coccolithus pelagicus and *Helicosphaera carteri* show both a parallel pattern along the section: maxima values of these species are observed in diatomites and in the upper marls, decreasing progressively along sapropels (Fig. 5). *Calcidsicus leptoporus* is always abundant at base and top of sapropels (decreasing in the middle part), as well as in diatomites, especially in UA8, where reach percentages close to 5% (Fig. 5).

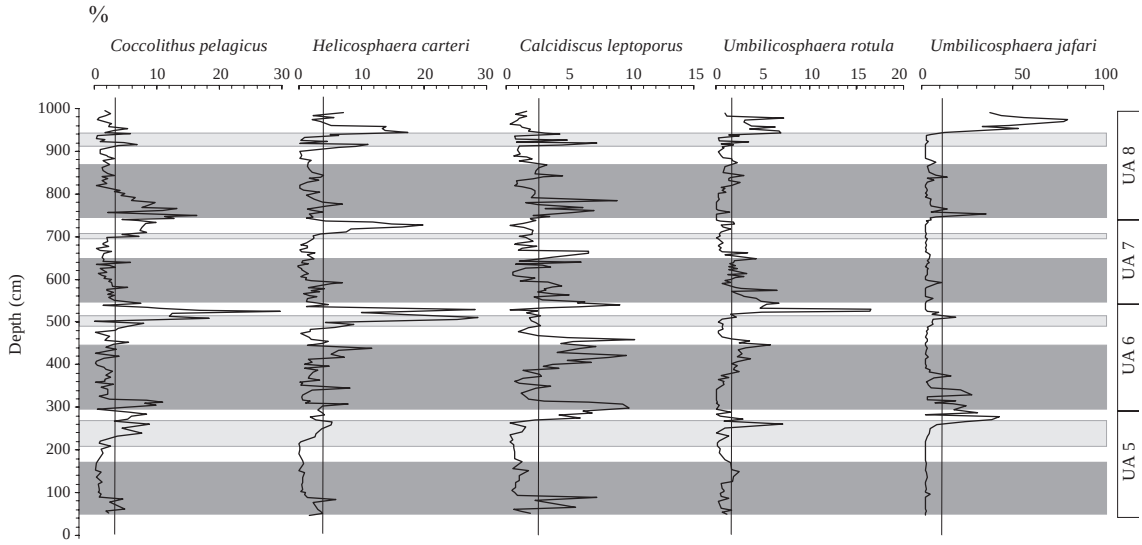

Fig. 5. Relative abundances (percentage) of some Coccolithophore species identified in the four analyzed cycles (Appendix B). The thin line crossing plots represents the media. Dark grey bands are sapropels, light grey bands are diatomites, white bands are marls.

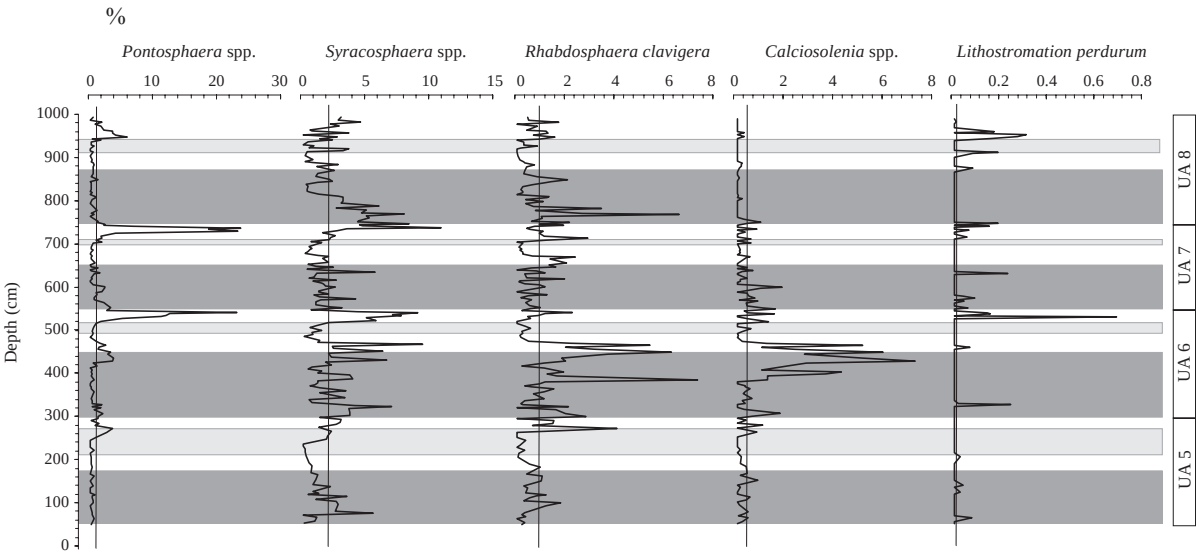

Fig. 6. Relative abundances (percentage) of miscellaneous species identified in the four analyzed cycles (Appendix B). The thin line crossing plots represents the media. Dark grey bands are sapropels, light grey bands are diatomites, white bands are marls.

Umbilicosphaera rotula present also a rhythmic pattern. This species increases from the base to the top of sapropels, and decreases from the lower marls to the top of diatomites, showing peaks close to the top of this lithology and in the upper marls. *Umbilicosphaera jafari* is very abundant (sometimes dominant) at the top of diatomites and in the upper marls and base of sapropels (in UA6 especially). This pattern is also followed by *Pontosphaera* spp., although significant peaks in the upper homogeneous marls of UA6 and UA7 are observed. *Syracosphaera* spp. show also peaks at these levels but it is also abundant in sapropels (Fig. 6).

Other taxa recorded regularly, such as *Rhabdosphaera clavigera, Calciosolenia* spp. or *Lithostromation perdurum*, show an irregular trend. Interestingly peaks of *Calciosolenia* spp. are observed in sapropels of UA6 (Fig. 6).

Taking into account the P/Ti record, previously described by Filippelli et al. (2003), maxima values occur in diatomites, with a close relationship with the opal record (Fig. 2).

Conversely, total organic matter (TOC, here expressed in weigh percentage) does not show a repetitive patter. Peaks in TOC occur in sapropels and low values in diatomites and homogenous marls within cycle UA5, whereas in UA6 and UA7 TOC is moderate in sapropels and increase in diatomites. In UA8 low TOC values occur in the sapropel and moderate values are found in the diatomite and homogeneous marl.

Regarding oxygen stable isotopes, in general the upper part of sapropels is characterized by light values, reaching slightly heavier values in diatomites and homogeneous marls. However, in UA5 this trend is less marked than in other cycles.

To better understand the relationship between calcareous nannofossil taxa, geochemical and other micropaleontological proxies and lithologies, and to summarize the data above, our quantitative results were regrouped in four semiquantitative categories and plotted in Fig. 7. From this visualization we can infer: sapropels are characterized by an assemblage where *Sphenolithus* and *Discoaster* are the most significant taxa. *Discoaster* mainly occurs in the upper half of the sapropels, reaching sometimes the lower marls, as may be seen in UA7. *R. rotaria* is also a characteristic component of this assemblage. The lower marls, although containing abundant *Discoaster* and *Sphenolithus*, and occasionally *Pontosphaera* and *Syracosphaera* (UA6 and UA7), are characterized by a dominance of small *Reticulofenestra. R. pseudoumbilicus* is abundant in the diatomites, whereas *C. pelagicus, H. carteri* and *U. jafari* are abundant in the upper marls.

4. Discussion

4.1. Paleoecological significance of some calcareous nannofossil taxa

Most of the species identified in the Messinian sediments are extinct, and their habitat are not always well understood. A comparison with some other micropaleontological data, mainly from planktonic foraminifers, provides valuable information. In Fig. 8 we synthesized some of the results from Sierro et al. (2003) and Pérez-Folgado et al. (2003). Three groups of planktonic foraminifers are here considered in relation with their habitat: "deep chlorophyll maximum (DCM) dwellers", mainly neogloboquadrinids; "cold-eutrophic", including *Globigerina bulloides* and *Turborotalita quinqueloba*; and "warm-oligotrophic", with *Globigerinoides obliquus*, *Globigerinoides sacculifer*, *Orbulina universa* and *Globigerina apertura* (Fairbanks and Wiebe, 1980; Fairbanks et al., 1982; Reynolds and Thunell, 1985; Sautter and Thunell, 1989; Rohling and Gieskes, 1989; Hemleben et al., 1989).

A comparison between the results plotted in Figs. 3–8, and additional data from geochemical

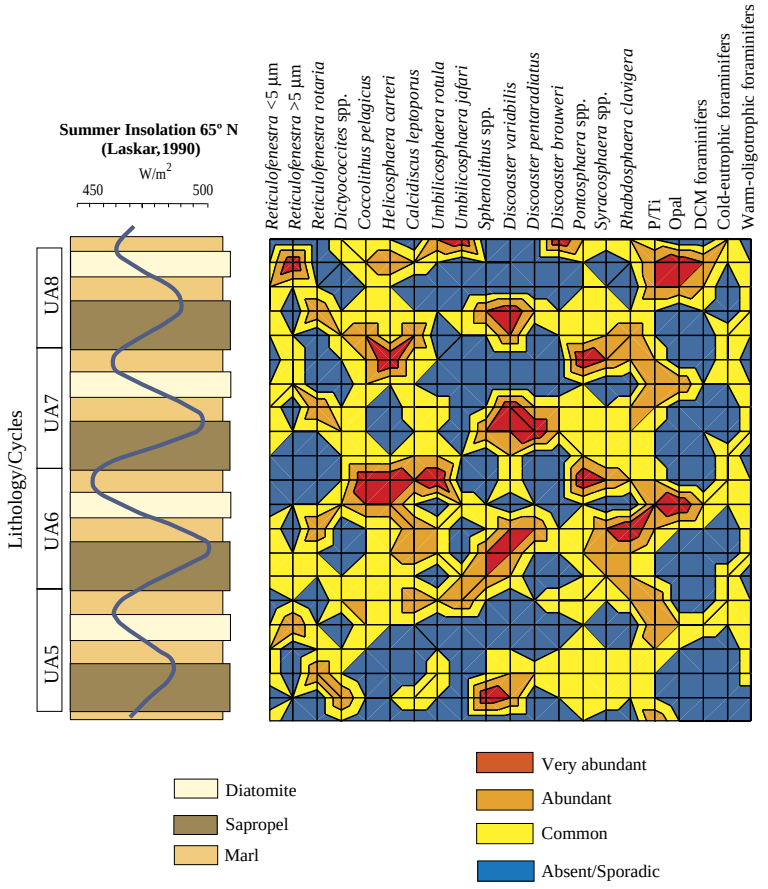

Fig. 7. Three-dimension projected plot synthesizing temporal distribution (succession) of the most significant calcareous nannofossil taxa, planktonic foraminifers groups, geochemical and sedimentological data for the four studied cycles (schematic; note the constant thickness) and their relationship with the insolation curve (Laskar, 1990). The semiquantitative categories are based on Figs. 2–7 and in the Appendix table. The defined categories are, for each taxon: (1) absent or sporadic: no record or mean values below the arithmetic median; (2) common (moderately abundant): with values close to the median; (3) abundant: values one time above the median; and (4) very abundant: with values several times the median; in this case we include the entire number of times represented. The same procedure is followed for planktonic foraminifers and for the P/Ti and Opal records. A reddish colour indicates higher relative concentration of a taxon (or compound or ratio), whereas a blue colour is related to low values or an absence.

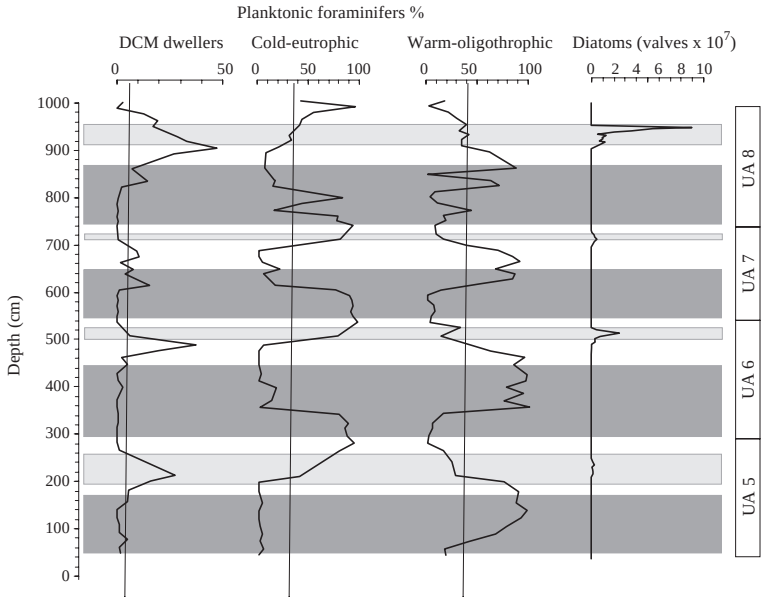

Fig. 8. Percentages of planktonic foraminifers grouped according to environmental characteristics (after Sierro et al., 2003 and Pérez-Folgado et al., 2003); details about characteristic and components of these groups are in text. The thin line crossing plots represents the media. Dark grey bands are sapropels, light grey bands are diatomites, white bands are marls.

proxies (Fig. 2), allow us to better understand the living conditions of some calcareous nannofossil taxa.

Discoaster is a genus traditionally considered an inhabitant of warm and oligotrophic waters (Lohmann and Carlson, 1981; Flores and Sierro, 1987; Flores et al., 1992, 1995; Chepstow-Lusty et al., 1989, 1992; Vázquez et al. 2000). In our samples *Discoaster variabilis* is the dominant species, with maxima at the end of sapropels. Taking into account the planktonic foraminifers we observe a correspondence with warm-oligotrophic species. In contrast, *Discoaster* shows an antagonistic trend with the "DCM group". These parameters coincide with low values in the P/Ti ratio, indicating that *Discoaster* sl. are warm-oligotrophic taxa that increase their abundance when pycnocline is deep. Although speculative, this pattern may indicate that *Discoaster's* behaviour is similar to that of *Florisphaera profunda*, a lower photic layer inhabitant of tropical and subtropical waters in the present day ocean (Okada and McIntyre, 1977; Molfino and MacIntyre, 1990), and abundant in recent sapropels (Negri et al., 1999a). Consequently we propose that *Discoaster* may have lived in the lower photic zone. This is especially significant in the case of *Discoaster pentaradiatus*, a warm species (Negri et al., 1999b) that peaks at the top of sapropels.

Sphenolithus spp. is also present in the sapropels and at the lower marls, and shows a similar trend as the warm-oligotrophic planktonic foraminifers. This is in agreement with previous observations by Haq and Lohmann (1976), Lohmann and Carlson (1981), Flores and Sierro (1987), Flores et al. (1995) and Castradori (1998).

Other species that show some correspondence with the warm-oligotrophic assemblage are *Syracosphaera* spp. and *Rhabdosphaera clavigera*. In similar cyclic materials, both from the Miocene and Pleistocene, Negri et al. (1999a,b), Negri and Giunta (2001) and Negri and Villa (2000) observed an increase of *Syracosphaera, Helicosphaera carteri* and *R. clavigera* and a decrease of *Coccolithus pelagicus* and *Discoaster pentaradiatus* in sapropel layers.

Special mention must be made of *Umbilicosphaera rotula* and *Umbilicosphaera jafari*. *U. rotula* shows small abundance peaks at the top of sapropels, but is most abundant immediately above diatomites. *U. jafari* shows peaks (sometimes more than 50% of the entire assemblage) just above the diatomites, replacing small *Reticulofenestra* (Fig. 4). As observed in Figs. 2

and 5, this occurs when the P/Ti ratio is still high, immediately after a peak of the diatom *Chaeotoceros* RS ("resting spores") (Pérez-Folgado et al., 2003). Although *U. jafari* is close to *Umbilicosphaera sibogae*, an inhabitant of the upper photic zone in tropical waters in mesotrophic and oligotrophic environments (Okada and McIntyre, 1979; Roth, 1994; Young, 1994), its behavior appears not to be related to temperature (it has no relation with the warm-oligotrophic assemblage of planktonic foraminifers). Maximum abundance occurs when silica is depleted in the system, immediately after the peaks of diatoms. Another explanation for the punctuated peaks of these species is an increase in salinity. Sierro et al. (2003) note that after diatomite deposition, the marls are characterized by heavy values of $\delta^{18}O$, which can be explained as a result of an increase in the evaporation/precipitation ratio (Fig. 2). These authors observed at these levels maxima in small specimens of the foraminifer *Globigerinita glutinata*, as a response to a "stressed" environment (increase of salinity or changes in the nutrient regime). Immediately after these peaks in the oxygen isotope record, *Discoaster brouweri* shows peaks in agreement with warm-oligotrophic conditions. However, the aforementioned peak of this species at the top of UA8 (Fig. 3) is due to abundant robust specimens with morphology close to *Discoaster intercalaris*, interpreted by Negri et al. (1999b) as a cool water species. Here, the observed increase in abundance is not well correlated with a relative decrease of surface water temperatures, but as result of the "stressed" conditions previously discussed.

Although the above mentioned taxa are abundant, the calcareous nannofossil assemblage is dominated by *Reticulofenestra*. Species smaller than 5 μm (*Reticulofenestra minuta* and *Reticulofenestra minutula*) are the most abundant types. These small species increase in the sapropels, attain maximum values at the lower marls, and decrease progressively from the base of diatomites. This reduction can be related with dilution, but our data support the idea that during diatomite deposition the ecological niche of calcareous nannoplankton is mainly occupied by diatoms (Fig. 8). This idea is in agreement with Negri and Villa (2000), who interpreted the reduction of coccolithophores as the result of ecological competition with diatoms. It is interesting to point out the good correlation between *Reticulofenestra* <5 μm and the planktonic foraminifers linked to the DCM. This indicates a close relationship, with increases of this morphotype related to a shallow although still weak nutricline, but under a situation that prevents the dominance of diatoms, just immediately before the increase in the P/Ti ratio. Unfortunately, with the data available it is unclear if nutrients other than P are limiting total calcareous nannofossil abundance across the lithotypes, and we do not have age control within the individual sapropel/marl couplets to calculate sedimentation rate and thus determine accumulation rate records of biological production.

Peaks of *Reticulofenestra pseudoumbilicus* (>5 μm) coincide with peaks in opal, diatoms and P/Ti, and cold-eutrophic foraminifers, showing a correspondence with high productivity and relatively cool conditions (Figs. 5, 7 and 8). *Reticulofenestra rotaria* is occasionally identified increasing its abundance significantly at the top of sapropels. As a probable inhabitant of the upper photic layer (as the closest present day species; Young, 1994), this species seems to increase in warm water conditions. During these episodes low values in the $\delta^{18}O$ in the planktonic fauna were observed by Sierro et al. (2003) and Pérez-Folgado et al. (2003), and we do not discount a relationship between the increase of this species with a reduction in salinity.

Coccolithus pelagicus is abundant in the upper marls and at the base of sapropel and show a direct relationship with the cold-eutrophic foraminifers. No correlation exists between *C. pelagicus* and the productivity indicator P/Ti, supporting the scenario outlined by Filippelli et al. (2003) that the diatomites represent the peak in nutrient input to surface waters, with the overlying marls deposited under conditions of lower net nutrient flux to the photic zone. The dominant morphotype identified here is *C. pelagicus* <10 μm; the *cool* subspecies *C. pelagicus* ssp. *pelagicus* (Geisen et al., 2002). Although in our material the abundance of *C. pelagicus* is low and the nannoflora assemblage is essentially warm, we observe slight variations such as a progressive reduction of this taxon from base to top of sapropel, similar to those observed by Negri et al. (2003) in Pleistocene sapropels.

Helicosphaera carteri has peaks in the upper marls when a decrease in P/Ti occurs. Negri et al. (1999a) noticed an increase of this species in sapropels, whereas Colmenero-Hidalgo et al. (2004) observed increases of this taxon related with iceberg melting episodes

during the last glacial period. Here *H. carteri* increase their abundance after diatomites, indicating an episode of relative high productivity and, as noted earlier, probably with enhanced salinities.

Other abundant species such as *Calcidiscus leptoporus* (Figs. 5 and 7) do not show a regular pattern here, and their distribution is neither correlated with lithology nor with some of the other proxies discussed here. In the same sense a controversy exists about the behavior of this taxon: some data indicate that this species is a warm and oligotrophic taxa (e.g., Geitznauer et al., 1977; Okada and McIntyre, 1977; Brand, 1994; Ziveri et al., 2000), whereas other reports link this taxon with high nutrient content and thus colder more eutrophic conditions (Young, 1994; Giraudeau, 1992; Flores et al., 2003).

In terms of calcareous nannofossil production we indicate the clear relationship with the calcium carbonate content. Maxima in the total abundance occur in the lower portion of the homogeneous marls, close to the predicted maxima insolation, when peaks in P/Ti reach moderate to high values (never the highest). The availability of nutrients such as silicon in the upper photic layer controls the composition of the phytoplanktonic assemblage. Mixing and consequent upwelling favors the regular increase of diatoms which compete with calcareous nannoplankton and become dominant, triggering diatomite deposition. Depletion of silicon, especially after diatomites UA5 and UA8, and availability of nutrients that can be used for calcareous nannoplankton, result in the development of opportunistic species not common in the regular mid and low latitude assemblages. Reaching a mesotrophic regime, the calcareous nannofossil assemblages increase in diversity and return to "normal" composition, dominated by small *Reticulofenestra*. As noted, changes in salinity can play also an important role in the characterization of assemblages.

4.2. Paleoenvironmental reconstruction

Micropaleontological and sedimentological data indicate that during the late Messinian, prior to the *Salinity Crisis*, the Sorbas basin had a warm tropical climate; the development of coral and algal reefs gives an excellent picture of this scenario (e.g. Martín and Braga, 1994). This area did have an interconnection between the adjacent basin and the open Mediterranean Sea, but this gateway certainly experienced changes in depth and width due to intense tectonic activity and sea level variations (e.g., Kouwenhoven et al., 1999; Sierro et al., 2001, 2003). The analysis of benthic foraminifers in the last cycles of the Lower Abad member and first of Upper Abad (UA1) indicates that these sediments were deposited under 1100 m in paleo-water depth (Krijgsman et al., submitted for publication), progressively shallowing towards the uppermost cycles (UA34) (Troesltra et al., 1980; Sierro et al., 1997, 2003). In units UA5 to UA8 the foraminifer assemblages observed by Sierro et al. (2003) and Pérez-Folgado et al. (2003) at these cycles are similar to the Lower Abad units, but with a reduction in the benthic fauna in the sapropel (indicating oxygen restriction at the bottom). Kouwenhoven (personal communication, 2005) studying samples from these cycles estimate a water column deeper than 400 m.

For every defined cycle the bottom of sapropel is consistent with a relatively cold surface water and the initial development of a stable pycnocline (thermocline), promoting the development of calcareous nannofossil assemblage characteristic of the lower photic zone. Further stabilization (upper half of sapropel) of the thermal and salinity structure resulted in stratification under a scenario of warmer sea surface temperature favoring the formation of a well developed permanent pycnocline with a deep nutricline. For equivalent sediments in adjacent basins, Sierro et al. (2000) analyzed a gamma-ray data set and concluded that for intervals of minimum precession (maximum summer insolation), an increase in runoff occurs. This is supported by lower $\delta^{18}O$ values (Pérez-Folgado et al., 2003) likely due to a freshening of surface waters, perhaps as a result of abrupt changes in the atmospheric system that produce an intensification in the African monsoons or stronger influence of the Atlantic depressions during periods of summer insolation maxima (Rossignol-Strick, 1985; Hilgen, 1991; Rohling and Hilgen, 1991). Extreme warm conditions in the upper photic zone allow the development of species like *Reticulofenestra rotaria*, only present at these levels; it is difficult to distinguish, however, if this is also the response to a decrease in salinity. This situation is especially significant during sapropels of UA6 and UA7, corresponding to maximum insolation from the studied cycles.

The deposition of the lower marls is marked by a decrease in insolation (increase in the precession index),

and a progressive reduction of mean temperatures. The calcareous plankton indicates a reduction in the surface water temperature and characterizes a relatively shallow DCM, a shoaling of the pycnocline and the onset of eutrophication. This situation is consistent with wind intensification (Sierro et al., 2003) and resultant upwelling of nutrient-rich deeper water, a fertilization process exacerbated by the accumulation of P in deep waters due to high reflux of P from bottom sediments under anoxic conditions during the interval of stratification (Filippelli et al., 2003). This process is combined with the oxygenation of the bottom that reduces the preservation of organic matter and formation of sapropels, although a weak stratification can occur.

Diatomite deposition occurred under conditions of minima insolation (maxima precession). At this time, a peak in upwelled nutrients occurs as mixing increases and benthically stored nutrients are injected into the photic zone at a high rate (Filippelli et al., 2003). A probable competition between primary producers takes place, with diatoms replacing the calcareous nannofossil niche. Although surface temperatures were lower than in the above mentioned levels, they were not cold enough to prevent the development of characteristic warm taxa. Pérez-Folgado et al. (2003) identified in the same material *Rhizosolenia* spp., *Thalassionema* spp. and *Chaeotoceros* RS. *Rhizosolenia* spp. as the dominant taxa in the middle and upper part of diatomites, being subsequently replaced by *Chaeotoceros* RS in the uppermost sector. *Chaeotoceros* RS reach higher concentrations in nutrient-rich surface waters of upwelling regimes, particularly at the onset of nutrient depletion after blooms (Abrantes, 1988; Bárcena and Abrantes, 1998).

The upper marls were deposited in a regime of similar oceanographic conditions as the diatomites, although we suggest a progressive increase in the temperature and stratification of surface waters. Peaks of *Umbilicosphaera jafari* could coincide with an increase in salinity, when depletion in some nutrients due partially to the exhaustion of the benthic P pool prevents the bloom of diatoms, in a mesotrophic environment. This situation is especially enhanced in units UA5 and UA8 at the time when insolation declines, but after reaching minimum values.

A generic interpretation of our results and those previously shown by Filippelli et al. (2003), Sierro et al. (2003) and Pérez-Folgado et al. (2003) are synthesized in Fig. 9.

5. Conclusions

The calcareous nannofossil assemblages identified in the alternating lithologies observed in the Sorbas basin during the late Messinian allow us to support the

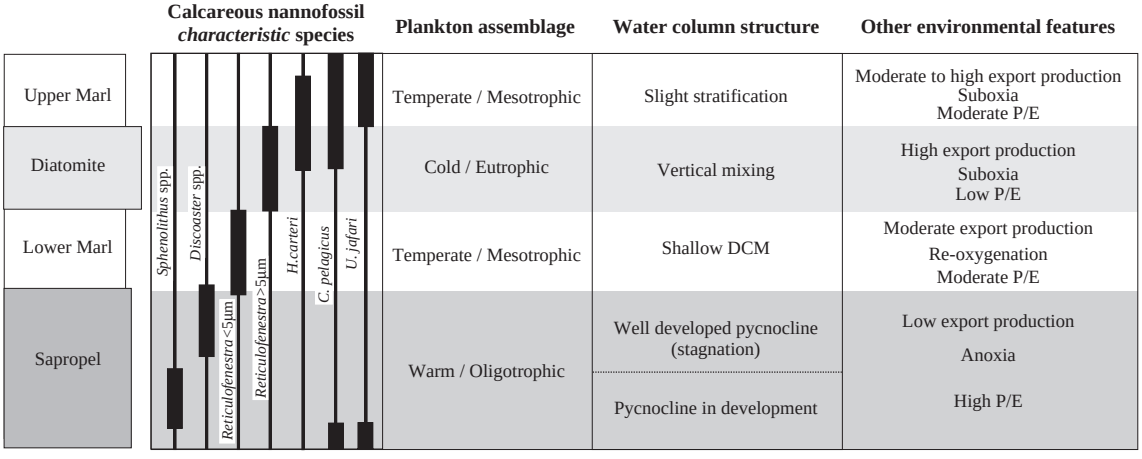

Fig. 9. Synthetic representation of a lithological cycle from the Upper Abad member in the Sorbas basin: main components of the calcareous nannofossil assemblages, general characteristic of the water column constituents and their relationship with other environmental features. The thick bars represent schematically peaks in abundance of the taxa. DCM=deep chlorophyll maximum; P/E=precipitation–evaporation ratio. This compilation is based in this study and completed with data from Filippelli et al. (2003), Sierro et al. (2003), and Pérez-Folgado et al. (2003).

hypothesis that the surface water dynamics are climatically (orbital) controlled. Maxima of phytoplanktonic productivity correspond to marls and diatomites, in a sedimentary scenario where a relatively shallow pycnocline increases the surface productivity and reduces the preservation of organic matter due to an intense reoxygenation in the bottom. This confirms, as previously reported, that the generation of sapropel–marl sequences is due to a combined process of production and preservation of organic matter.

Paleoenvironments corresponding to sapropel deposition responded to oligotrophic conditions: calcareous nannofossils were the dominant phytoplanktonic organisms, which together with foraminifers and perhaps other non-fossilized organisms provided the organic matter. A well developed pycnocline, with a nannoplanktonic community living in the lower photic zone, coexist with an anoxic environment at the bottom.

The high resolution analysis of calcareous nannofossil assemblages and their comparison with other proxies shed light on the paleoecological context of several taxa. *Sphenolithus* spp. and *Discoaster* sl. are confirmed as warm-oligotrophic genera; and the species *Discoaster pentaradiatus* is indicator of most extreme conditions. Moreover, we suggest that *Discoaster* was a lower photic zone inhabitant based on our observations of an inverse correspondence with DCM dweller foraminifers. As a major component of the assemblages, small *Reticulofenestra* is linked to a relatively shallow DCM, with a stable but also shallow thermocline. Conversely, other taxonomically similar species such as *Reticulofenestra pseudoumbilicus* (>5 μm) are more frequent under conditions of extreme mixing in the basin. In contrast, another reticulofenestrid, *Reticulofenestra rotaria*, show peaks at the top of sapropels, here interpreted not only as due to an increase of surface water temperature, but also to decreasing salinity.

Umbilicosphaera jafari replaces small *Reticulofenestra* after diatomites, and although this is not well understood, we observe that these peaks coincide with strong variations in the $\delta^{18}O$ isotope record, indicating a possible increase in salinity.

Acknowledgements

The authors wish to express their thanks to Dr. Elisabetta Erba and Dr. Kay Emeis for their valuable and critical comments. Research grants REN2003-08642-C02-02 CLI, BTE 2002-04670 (Ministerio de Educación y Ciencia) and Junta de Castilla y León SA088/04 supported this study. Support was also provided by the Petroleum Research Fund through Donors to the American Chemical Society, and the US National Science Foundation. Thanks are due to Jesús Roncero and José Gravalosa for technical assistance in sample processing.

Appendix A. Taxonomic appendix

Calcareous Nannofossils
Calcidiscus leptoporus Murray and Blackman, 1898
Calciosolenia Gran, 1912
Coccolithus pelagicus (Wallich, 1877)
Dictyococcites antarcticus Haq, 1976=*Reticulofenestra antarctica* (Haq, 1976)
Discoaster brouweri Tan, 1927, emend. Bramlette and Riedel, 1954
Discoaster intercalaris Bukry, 1971
Discoaster pentaradiatus Tan, 1927, emend. Bramlette and Riedel, 1954
Discoaster variabilis Martini and Bramlette, 1963
Florisphaera profunda Okada and McIntyre, 1980
Helicosphaera carteri (Wallich, 1877)
Lithostromation perdurum Deflandre, 1942
Pontosphaera Lohmann, 1902
Reticulofenestra minuta Roth, 1970. Included in this study in *Reticulofenestra* <5 μm.
Reticulofenestra minutula (Gartner, 1967). Included in this study in *Reticulofenestra* <5 μm.
Reticulofenestra pseudoumbilicus (Gartner, 1967). Included in this study in *Reticulofenestra* >5 μm.
Reticulofenestra rotaria Theodoridis, 1984
Rhabdosphaera clavigera Murray and Blackman, 1898
Sphenolithus abies Deflandre in Deflandre and Fert, 1954
Sphenolithus neoabies Bukry and Bramlette, 1969
Syracosphaera Lohmann, 1902
Umbilicosphaera rotula (Kkamptner, 1956)
Umbilicosphaera jafari Müller, 1974
Planktonic foraminifers
Globigerina apertura Cushman,1918
Globigerina bulloides (d'Orbigny, 1826)
Globigerinita glutinata (Egger, 1895)
Globigerinoides obliquus Bollii, 1957
Globigerinoides sacculifer (Brady, 1877)
Orbulina universa d'Orbigny, 1839
Turborotalita quinqueloba (Natland, 1938)
Diatoms
Chaetoceros (Ehrenberg 1844)
Rhizosolenia Ehrenberg 1841
Thalassionema (Heiden, 1928)

Appendix B. Calcareous nannofossil species abundance in the Sorbas basin

Depth (cm)	*Reticulofenestra* <5%	*Reticulofenestra* >5%	*Dictyococcites* (%)	*C. pelagicus* <10%	*C. pelagicus* >10%	*H. carteri* (%)	*C. leptoporus* (%)	*C. macintyrei* (%)	*Sphenolithus* (%)	*D. variabilis* (%)	*D. pentaradiatus* (%)	*D. brouweri* (%)	Total *Discoaster* (%)	*Pontosphaera* (%)
992.04	40.33	3.82	0.00	1.74	0.00	7.30	1.39	0.00	0.70	0.70	0.00	3.82	4.52	0.49
986.35	40.59	3.52	0.00	2.56	0.00	2.36	0.45	0.00	1.09	0.64	0.03	2.88	3.55	0.00
980.66	9.46	3.51	0.00	1.76	0.00	5.81	1.35	0.00	1.35	0.07	0.00	7.57	7.64	1.76
976.39	6.68	2.30	1.46	0.73	0.00	2.30	0.73	0.00	0.83	0.31	0.00	1.98	2.30	0.73
972.12	4.92	4.18	0.00	0.39	0.00	3.59	0.64	0.00	0.20	0.08	0.00	1.61	1.69	1.62
963.58	34.62	4.15	1.11	2.77	0.00	5.26	0.01	0.00	0.55	0.01	0.00	0.06	0.06	2.05
959.31	30.55	7.64	0.00	2.35	0.00	14.10	0.82	0.00	0.00	0.59	0.00	0.88	1.47	3.53
955.04	13.12	5.55	0.00	2.32	0.00	13.43	1.01	0.00	0.50	0.30	0.00	0.61	0.91	3.53
950.77	28.00	8.00	1.33	5.33	0.00	14.00	1.67	0.00	0.07	0.08	0.00	0.33	0.41	4.00
946.50	33.51	13.71	0.00	3.05	0.00	17.51	1.52	0.46	1.98	0.46	0.00	0.24	0.70	5.71
943.00	72.08	9.57	0.00	1.59	0.00	5.10	2.87	0.00	0.38	1.28	0.00	0.38	1.66	0.36
939.50	50.00	25.49	0.00	5.72	0.00	6.54	4.08	0.00	0.46	0.00	0.00	0.00	0.00	1.63
936.00	91.44	5.05	0.00	0.40	0.00	1.01	0.40	0.00	0.12	0.06	0.00	0.00	0.06	0.10
929.00	92.29	5.05	0.00	0.34	0.00	0.44	0.44	0.00	0.26	0.04	0.00	0.13	0.17	0.16
925.50	58.08	22.12	0.00	1.71	0.00	4.70	4.70	0.00	1.58	0.00	0.00	0.00	0.00	0.61
922.00	92.14	4.25	0.16	0.88	0.00	0.33	0.56	0.00	0.07	0.07	0.00	0.00	0.07	0.16
918.22	34.40	36.77	0.00	4.74	0.00	11.15	7.12	0.00	0.00	0.47	0.00	0.00	0.47	0.00
914.45	51.01	23.19	0.00	6.86	0.00	9.27	4.27	0.00	0.00	1.06	0.00	0.52	1.58	0.00
910.68	75.40	10.99	0.38	3.79	0.00	6.44	0.76	0.00	0.00	0.76	0.00	0.17	0.92	0.38
902.12	95.56	1.41	0.00	0.85	0.00	0.38	0.62	0.00	0.43	0.13	0.00	0.00	0.13	0.06
893.56	93.07	2.30	0.00	0.92	0.00	0.64	0.86	0.00	0.18	0.13	0.00	0.09	0.22	0.29
889.20	93.70	1.42	0.06	1.94	0.00	0.45	0.32	0.00	0.48	0.26	0.00	0.00	0.26	0.10
885.00	89.12	2.27	0.00	2.11	0.00	0.38	1.39	0.00	0.39	0.76	0.00	0.08	0.83	0.45
881.00	75.86	6.52	0.00	3.14	0.00	2.17	1.79	0.00	0.97	0.24	0.00	0.14	0.39	0.60
875.75	82.43	2.38	0.20	1.39	0.00	1.71	0.79	0.00	0.91	0.16	0.00	0.00	0.16	0.40
867.63	77.41	4.54	0.00	2.42	0.30	1.51	3.02	0.00	1.63	3.33	0.00	0.00	3.33	0.42
859.50	87.32	0.97	0.19	1.16	0.00	1.82	2.33	0.00	1.16	0.61	0.00	0.08	0.69	0.39
853.00	83.66	1.45	0.00	1.31	0.00	2.28	2.09	0.00	2.42	0.97	0.00	0.15	1.12	0.15
846.50	61.15	4.50	0.00	2.07	0.00	4.05	2.07	0.00	4.23	4.95	1.35	0.22	6.52	1.17
842.55	57.06	2.76	0.00	3.22	0.46	3.68	4.33	0.00	5.98	3.41	0.00	0.92	4.33	0.05
838.60	82.77	2.25	0.00	1.25	0.00	1.75	2.75	0.00	1.85	1.30	0.00	0.10	1.40	0.20
834.70	77.59	2.11	0.00	2.11	0.00	3.28	1.88	0.00	3.05	1.99	0.00	0.12	2.11	0.14
830.80	88.20	1.70	0.62	1.23	0.00	1.54	0.52	0.00	1.76	0.86	0.00	0.00	0.86	0.15
823.00	91.30	1.23	0.62	2.00	0.00	0.31	0.62	0.00	1.23	0.77	0.00	0.00	0.77	0.19
819.10	95.65	1.29	0.55	0.37	0.00	0.37	0.37	0.00	0.68	0.05	0.00	0.03	0.08	0.00
815.20	91.31	1.84	0.00	1.01	0.00	0.34	1.01	0.00	0.25	1.59	0.00	0.10	1.69	0.25
811.30	86.88	2.84	0.47	2.60	0.00	0.95	1.75	0.00	0.85	1.18	0.00	0.00	1.18	0.00
807.40	72.94	4.02	0.50	4.02	0.00	3.52	2.01	0.00	4.73	2.41	0.00	0.00	2.41	0.80
803.50	73.45	5.86	0.00	3.24	0.00	2.76	2.07	0.00	4.62	1.79	0.00	0.41	2.21	0.90
799.60	73.75	3.81	0.00	4.85	0.00	1.39	2.08	0.00	7.27	1.66	0.00	0.00	1.66	0.35
795.70	79.96	5.38	0.00	4.23	0.77	1.92	1.92	0.00	0.54	0.54	0.00	0.00	0.54	0.12
789.90	72.19	9.17	1.15	6.53	0.00	2.64	1.72	0.00	0.32	0.65	0.16	0.14	0.96	0.00
784.00	62.22	6.38	0.00	5.90	0.00	3.99	8.77	0.00	0.80	2.07	0.00	0.26	2.33	0.48
779.20	60.04	9.14	1.31	9.66	1.57	7.05	1.31	0.00	0.00	1.85	0.00	0.00	1.85	0.78
774.60	67.26	5.23	1.49	8.97	0.00	4.48	2.24	0.00	0.90	1.20	0.00	0.00	1.20	1.05

(continued on next page)

Appendix B (*continued*)

Depth (cm)	*Reticulofenestra* <5%	*Reticulofenestra* >5%	*Dictyococcites* (%)	*C. pelagicus* <10%	*C. pelagicus* >10%	*H. carteri* (%)	*C. leptoporus* (%)	*C. macintyrei* (%)	*Sphenolithus* (%)	*D. variabilis* (%)	*D. pentaradiatus* (%)	*D. brouweri* (%)	Total *Discoaster* (%)	*Pontosphaera* (%)
768.40	51.11	8.27	0.00	7.52	0.75	1.50	6.01	0.00	1.50	2.71	0.24	1.05	4.00	0.17
765.20	49.23	5.47	1.09	13.13	0.00	2.19	2.84	0.00	1.09	1.55	0.00	0.48	2.04	0.66
760.60	56.44	5.94	0.99	10.89	0.00	3.96	6.93	0.00	2.38	2.77	0.00	0.00	2.77	0.00
756.00	43.98	2.59	0.00	2.07	0.00	1.76	5.17	0.00	0.31	3.52	0.00	0.29	3.81	0.41
749.50	56.63	7.68	2.88	16.32	0.96	2.50	1.92	0.00	0.38	0.84	0.00	0.00	0.84	1.15
746.25	66.72	6.32	0.00	11.24	0.00	1.40	3.23	0.00	0.00	0.28	0.00	0.00	0.28	1.05
743.00	54.92	11.21	3.36	12.78	0.00	3.36	1.68	0.00	1.12	0.27	0.00	0.09	0.36	2.24
739.75	71.62	6.58	0.73	4.38	0.00	4.38	1.75	0.00	0.88	0.61	0.00	0.00	0.61	2.19
736.50	52.00	9.84	0.00	7.03	0.00	11.95	2.11	0.00	0.42	0.98	0.00	0.42	1.41	6.68
733.25	19.55	13.69	0.00	9.78	0.00	15.05	1.47	0.00	1.96	0.49	0.00	0.00	0.49	23.46
729.13	36.86	10.75	0.00	8.19	0.00	19.97	1.02	0.00	0.20	0.05	0.00	0.00	0.05	18.43
725.00	39.23	7.85	0.00	7.85	0.00	16.74	0.00	0.00	0.52	0.10	0.00	0.00	0.10	23.01
720.00	64.36	9.32	0.44	7.55	0.44	8.43	1.11	0.00	0.62	0.27	0.00	0.00	0.27	3.99
715.00	68.38	8.21	0.00	7.33	0.00	7.66	1.86	0.00	0.33	0.11	0.00	0.27	0.38	1.64
710.00	65.27	11.62	0.00	8.40	0.00	3.58	1.79	0.00	0.89	0.29	0.00	0.21	0.50	1.79
705.00	76.42	10.15	0.60	4.42	0.00	2.39	1.79	0.00	0.00	0.00	0.00	0.00	0.00	0.90
700.91	77.92	7.87	0.00	7.08	0.00	2.60	0.79	0.00	0.39	0.12	0.04	0.00	0.16	1.81
696.78	85.86	4.26	0.00	1.95	0.00	2.48	1.31	0.00	0.35	0.11	0.00	0.11	0.21	0.50
688.52	89.17	3.51	0.00	2.08	0.00	1.42	1.88	0.00	0.33	0.19	0.00	0.00	0.19	0.13
684.39	93.37	2.23	0.00	1.39	0.00	0.46	0.62	0.00	0.15	0.02	0.02	0.01	0.05	0.12
680.26	92.50	2.07	0.00	1.34	0.00	1.55	0.41	0.00	0.06	0.14	0.00	0.00	0.14	0.41
676.13	86.77	5.14	0.18	2.23	0.00	1.52	2.23	0.00	0.35	0.02	0.00	0.00	0.02	0.20
672.00	96.48	0.74	0.00	0.25	0.00	0.25	0.98	0.00	0.17	0.00	0.00	0.00	0.00	0.04
668.50	90.44	2.58	0.11	0.90	0.00	0.67	0.67	0.00	0.73	0.45	0.00	0.06	0.51	0.28
664.75	57.72	4.66	0.00	2.65	0.00	2.65	6.45	0.00	5.52	6.45	2.15	0.54	9.14	0.14
661.00	70.61	3.10	1.16	1.55	0.00	1.55	6.44	0.00	2.72	3.34	1.32	1.32	5.97	0.22
651.26	65.63	4.61	0.00	1.15	0.29	2.65	3.45	0.00	1.96	5.76	1.44	1.73	8.92	0.81
646.40	81.00	3.84	1.54	1.54	0.00	0.77	2.30	0.00	1.54	3.45	0.61	0.31	4.38	0.00
642.78	79.42	3.16	0.40	1.34	0.00	0.55	0.79	0.00	1.03	3.16	2.77	0.79	6.72	0.08
639.16	58.43	9.03	0.00	5.70	0.00	1.66	5.80	0.00	1.43	2.61	7.60	1.19	11.40	1.24
635.54	83.51	3.67	1.53	0.31	0.31	0.00	0.43	0.00	0.92	4.74	1.38	1.38	7.49	0.00
631.92	84.72	1.78	0.00	2.37	0.00	0.00	2.67	0.00	0.36	3.26	0.59	0.00	3.85	0.08
628.30	62.62	8.39	0.00	3.35	0.00	0.56	3.35	0.78	2.57	2.24	3.13	0.93	6.30	1.45
624.68	85.93	3.82	1.59	0.95	0.00	0.64	1.27	0.00	0.45	1.27	0.38	0.19	1.85	0.64
617.44	71.68	10.35	0.40	1.99	0.00	1.59	0.24	0.00	6.37	1.19	0.80	0.00	1.99	0.20
613.82	85.01	4.82	0.00	0.63	0.00	1.05	0.21	0.00	2.72	0.42	0.29	0.00	0.71	0.29
610.20	85.45	3.82	0.42	1.19	0.00	0.42	0.25	0.00	2.54	0.21	0.00	0.00	0.21	0.00
606.58	81.33	4.20	1.53	1.76	0.00	1.34	0.53	0.00	6.49	0.61	0.76	0.00	1.37	0.00
602.96	84.10	2.36	0.00	1.48	0.00	1.18	2.07	0.00	2.95	1.94	0.09	0.00	2.03	0.30
599.34	77.68	3.44	1.37	2.75	0.00	2.06	1.72	0.00	6.19	0.17	0.01	0.00	0.19	0.48
595.72	61.66	1.72	0.25	2.21	0.00	7.12	0.84	0.00	6.04	2.70	0.00	0.37	3.07	2.31
592.10	66.21	1.67	0.31	2.78	0.00	5.26	3.09	0.00	4.95	2.23	0.00	0.37	2.60	2.29
584.86	83.42	1.01	0.00	2.82	0.00	1.61	4.23	0.00	0.00	1.09	0.02	0.48	1.59	1.81
581.24	76.56	1.43	0.20	5.32	0.00	4.30	3.48	0.00	0.51	2.56	0.04	0.02	2.62	0.94
577.62	78.44	1.71	0.26	1.98	0.00	2.11	2.77	0.13	0.34	1.25	0.00	0.13	1.38	1.05
574.00	84.93	0.74	0.00	2.02	0.00	3.49	2.94	0.00	0.05	1.10	0.00	0.00	1.10	0.85
570.10	86.15	2.12	0.14	3.10	0.00	0.85	2.26	0.00	0.14	0.34	0.00	0.00	0.34	0.65

566.20	82.10	1.37	0.17	2.05	0.00	1.88	3.59	0.00	0.08	0.68	0.00	0.00	0.68	0.55
562.38	79.90	1.42	0.00	3.25	0.00	3.05	4.88	0.00	0.20	0.58	0.00	0.00	0.58	1.02
558.56	80.38	0.98	0.42	2.24	0.00	1.57	1.96	0.00	0.42	0.12	0.00	0.00	0.12	2.16
550.92	81.81	0.76	0.19	3.25	0.00	1.34	2.68	0.00	0.27	0.22	0.00	0.00	0.22	2.68
547.10	66.69	2.90	0.00	6.09	0.00	3.77	6.15	0.00	0.00	0.46	0.00	0.00	0.46	3.25
543.28	65.53	2.30	0.38	7.36	0.00	4.83	5.52	0.00	0.28	0.61	0.00	0.00	0.61	3.07
539.46	78.63	0.60	0.30	1.40	0.00	1.30	9.03	0.00	0.05	0.16	0.00	0.02	0.18	2.61
535.64	17.84	2.97	0.00	5.95	0.00	13.38	3.96	0.00	0.50	1.59	0.00	0.00	1.59	16.15
531.82	14.94	0.75	0.75	10.46	0.00	28.39	2.99	0.00	0.60	1.30	0.00	0.00	1.30	12.40
528.21	25.84	2.09	0.70	16.76	0.00	17.46	0.00	0.00	0.00	0.81	0.00	0.00	0.81	11.87
524.61	18.71	3.83	0.00	29.76	0.00	10.20	2.30	0.00	0.43	2.55	0.00	0.00	2.55	11.05
521.00	50.73	1.78	0.44	12.46	0.00	16.91	1.33	0.00	0.32	0.00	0.00	0.00	0.00	5.07
515.00	25.09	3.76	0.00	11.92	0.00	28.86	2.51	0.00	0.00	0.38	0.13	0.00	0.50	1.63
509.00	36.63	7.85	0.65	18.31	0.00	25.51	1.57	0.00	0.98	0.48	0.00	0.16	0.65	0.98
503.00	40.69	41.21	1.05	0.00	4.21	4.38	1.75	0.70	0.21	0.56	0.00	0.00	0.56	0.56
497.00	65.15	4.77	0.26	7.94	0.00	9.00	2.12	0.00	3.02	0.53	0.05	0.00	0.58	0.42
491.00	72.27	6.79	0.00	5.25	0.00	5.87	2.47	0.00	1.85	0.62	1.05	0.00	1.67	0.37
485.00	82.52	3.54	0.22	3.76	0.00	1.99	1.55	0.00	2.21	0.44	0.13	0.00	0.58	0.44
480.50	88.33	1.49	0.12	3.35	0.00	1.98	1.17	0.00	1.36	0.30	0.10	0.00	0.40	0.37
476.00	95.51	0.79	0.16	0.16	0.00	0.43	0.71	0.00	0.75	0.01	0.06	0.00	0.06	0.00
467.00	83.95	1.41	0.00	2.47	0.00	1.77	2.30	0.18	1.06	1.48	0.92	0.07	2.47	0.88
462.50	72.35	1.17	0.00	1.93	0.00	2.05	4.69	0.00	0.76	4.54	2.20	0.00	6.74	1.46
458.00	40.86	1.61	0.00	1.61	0.54	4.84	10.22	0.00	2.69	4.09	5.16	0.43	9.68	2.47
453.00	66.43	1.62	0.00	5.51	0.00	3.89	5.18	0.65	1.30	3.73	2.43	0.32	6.48	1.30
448.00	68.89	4.64	0.77	3.10	0.00	1.55	4.18	0.00	0.62	0.77	0.77	0.00	1.55	1.24
443.00	38.82	1.76	0.00	1.76	0.00	11.76	7.06	0.00	5.53	5.00	0.00	2.06	7.06	3.18
438.00	58.56	5.01	0.00	3.50	0.00	6.51	5.71	0.00	2.50	2.80	0.40	0.80	4.00	2.70
428.00	68.79	1.37	0.00	0.16	0.00	5.32	3.84	0.00	0.82	3.45	0.03	0.55	4.03	3.67
421.90	42.99	4.56	0.00	3.91	0.00	7.43	9.51	0.00	4.82	3.91	0.00	0.21	4.12	3.52
415.80	73.66	3.43	0.00	1.46	0.00	1.71	8.14	0.00	0.26	1.54	0.00	0.00	1.54	0.51
409.70	78.93	3.01	0.00	0.33	0.00	2.34	4.68	0.00	1.54	1.20	0.00	0.33	1.54	1.00
405.12	82.73	1.81	0.00	0.20	0.00	1.01	6.64	0.00	0.52	1.01	0.00	0.00	1.01	0.00
400.54	76.85	1.86	0.00	0.52	0.00	4.97	3.49	0.00	2.23	3.90	0.37	0.00	4.27	0.32
395.96	81.79	0.81	0.19	1.44	0.00	1.06	2.69	0.00	0.31	1.63	0.38	0.13	2.13	0.18
391.38	73.65	2.85	1.07	1.78	0.00	3.20	3.99	0.00	1.07	2.56	0.00	0.28	2.85	0.30
386.80	60.04	4.87	1.62	2.84	0.00	2.43	1.05	0.81	11.76	3.45	1.01	0.41	4.87	0.20
377.64	59.87	3.95	0.30	1.82	0.00	1.82	2.43	0.00	0.97	0.91	0.71	0.12	1.74	0.61
373.06	76.36	4.24	0.85	2.55	0.00	1.70	2.55	0.00	2.26	0.90	0.90	0.00	1.81	0.17
368.48	77.14	3.13	0.00	1.74	0.00	3.47	1.04	0.00	6.25	1.39	0.69	0.00	2.08	0.00
363.90	88.08	4.77	0.33	1.64	0.00	0.23	0.70	0.00	1.26	0.20	0.13	0.00	0.33	0.00
359.32	92.19	1.78	0.45	0.15	0.00	0.74	0.39	0.00	1.28	0.34	0.08	0.00	0.43	0.09
354.74	84.71	2.51	0.00	3.01	0.00	0.50	0.75	0.00	1.15	1.10	0.35	0.00	1.45	0.15
349.31	51.11	6.11	0.00	1.11	0.00	8.33	3.33	0.00	17.78	2.44	0.67	0.00	3.11	0.56
343.88	65.06	0.63	0.21	2.09	0.00	2.34	2.09	0.21	4.60	0.92	0.21	0.00	1.13	0.42
333.03	60.71	2.91	0.73	2.18	0.00	0.73	0.91	0.00	1.45	0.15	0.00	0.00	0.15	0.22
327.60	91.15	1.78	0.00	0.76	0.00	0.56	1.16	0.00	1.89	0.31	0.00	0.07	0.38	0.33
321.00	89.70	1.66	0.00	2.43	0.00	0.76	1.43	0.00	1.43	0.07	0.00	0.02	0.09	0.33
317.55	57.89	5.91	0.59	8.27	0.59	2.01	1.54	0.00	1.48	0.83	0.00	0.83	1.65	1.77
314.10	58.82	2.43	0.00	10.92	0.00	1.21	2.79	0.00	8.49	2.43	0.00	1.21	3.64	0.36
310.65	41.09	8.06	0.00	8.06	0.00	8.06	6.45	0.81	0.97	2.42	0.00	0.26	2.67	1.61

(continued on next page)

Appendix B (*continued*)

Depth (cm)	*Reticulofenestra* <5%	*Reticulofenestra* >5%	*Dictyococcites* (%)	*C. pelagicus* <10%	*C. pelagicus* >10%	*H. carteri* (%)	*C. leptoporus* (%)	*C. macintyrei* (%)	*Sphenolithus* (%)	*D. variabilis* (%)	*D. pentaradiatus* (%)	*D. brouweri* (%)	Total *Discoaster* (%)	*Pontosphaera* (%)
307.20	31.70	12.55	2.64	9.91	0.66	3.96	9.25	0.40	0.08	2.64	0.00	0.00	2.64	0.66
298.60	52.53	6.11	1.22	0.49	0.00	3.18	9.77	0.00	2.03	1.22	0.00	0.00	1.22	1.95
290.00	38.87	3.97	0.36	5.66	0.00	3.97	6.02	0.00	0.60	1.32	0.00	0.36	1.68	1.20
285.25	24.62	5.47	1.64	3.61	0.00	1.86	2.95	0.00	0.44	0.33	0.77	2.52	3.61	0.55
280.50	36.14	5.16	0.00	5.90	0.00	1.92	3.98	0.00	0.44	0.38	0.00	0.09	0.47	0.18
274.66	34.08	6.33	0.00	5.32	0.00	2.88	5.75	0.00	0.00	0.29	0.00	0.07	0.36	1.44
268.83	55.43	5.18	1.55	3.11	0.00	5.49	2.07	0.00	1.04	0.06	0.05	0.05	0.17	0.73
263.00	58.00	4.39	0.88	8.79	0.00	5.27	0.00	0.00	0.88	0.26	0.09	0.00	0.35	3.51
253.00	64.49	16.60	1.28	4.47	0.00	3.83	1.28	0.00	0.00	0.20	0.06	0.13	0.40	2.55
241.00	58.07	23.80	0.00	7.62	0.00	2.86	0.95	0.00	0.95	0.42	0.57	0.00	0.99	0.95
235.20	63.02	25.75	0.00	3.60	0.00	2.70	0.00	0.00	0.00	0.23	0.00	0.11	0.34	0.00
223.60	95.63	1.90	0.02	0.88	0.00	0.44	0.22	0.00	0.07	0.13	0.04	0.01	0.18	0.07
219.73	97.75	1.07	0.13	0.72	0.00	0.08	0.00	0.00	0.08	0.03	0.00	0.13	0.16	0.00
212.00	92.41	2.06	0.23	2.52	0.00	0.23	0.27	0.00	0.69	0.00	0.23	0.00	0.23	0.59
204.00	95.27	0.98	0.21	1.05	0.00	0.28	0.28	0.00	1.27	0.04	0.04	0.04	0.11	0.04
196.00	94.77	1.40	0.06	1.40	0.00	0.22	0.38	0.00	0.47	0.02	0.19	0.06	0.27	0.13
180.00	92.56	1.13	0.11	0.68	0.00	0.79	0.38	0.00	0.45	1.02	0.29	0.27	1.58	0.11
172.00	88.90	1.68	0.42	0.28	0.14	0.84	0.98	0.00	0.63	0.49	0.49	0.56	1.54	0.28
156.00	91.43	2.36	0.00	0.14	0.00	0.14	0.24	0.00	1.06	0.47	0.20	0.28	0.95	0.07
150.33	84.90	2.18	0.33	1.00	0.00	1.00	1.51	0.33	0.50	0.92	0.59	0.50	2.01	0.67
139.00	83.91	1.97	0.25	0.25	0.00	0.74	0.74	0.00	2.95	2.21	0.84	0.00	3.05	0.00
128.50	87.87	1.02	0.27	1.25	0.00	0.76	0.76	0.00	1.25	0.76	1.14	0.00	1.90	0.49
123.25	92.50	1.92	0.64	0.64	0.00	0.64	0.43	0.00	0.00	0.17	0.34	0.00	0.51	0.00
112.75	93.79	0.97	0.00	0.73	0.00	0.73	0.48	0.00	0.73	0.24	0.19	0.05	0.48	0.00
107.50	84.46	4.22	0.80	0.80	0.40	0.40	0.20	0.00	4.38	1.00	0.16	0.00	1.16	0.80
103.75	89.06	2.45	0.15	0.59	0.00	1.18	0.15	0.00	1.57	0.10	2.36	0.00	2.47	0.30
100.00	81.61	2.30	0.00	1.02	0.00	1.02	0.38	0.00	3.58	0.26	1.74	0.36	2.35	0.26
92.50	86.53	3.86	1.47	0.81	0.92	1.47	0.64	0.00	1.29	0.48	1.36	0.00	1.84	0.46
88.75	59.09	4.58	0.00	4.58	0.51	6.11	7.13	0.00	7.64	3.67	0.00	0.51	4.18	0.51
81.25	66.14	9.45	5.31	2.36	0.00	2.36	2.01	0.00	10.63	2.72	0.00	0.00	2.72	0.00
65.50	51.27	6.48	1.08	4.86	0.00	3.24	5.40	0.00	22.13	1.94	0.00	0.65	2.59	0.27
60.50	75.01	7.23	1.36	1.81	0.00	3.62	0.27	0.00	1.81	2.08	0.00	0.00	2.08	0.27

Appendix B (*continued*)

Depth (cm)	*Syracosphaera* (%)	*G. rotula* (%)	*G. jafari* (%)	*R. clavigera* (%)	*Calciosolenia* (%)	*R. rotaria* (%)	*L. perdurum* (%)	*H. macroporus* (%)	*Amaurolithus* (%)	*Reticulofenestra* <5/g	*Reticulofenestra* >5/g	*Dictyococcites* (/g)	*C. pelagicus* <10/g	*C. pelagicus* >10/g	*H. carteri* (/g)	*C. leptoporus* (/g)	*C. macintyrei* (/g)
992.04	2.96	0.87	35.47	0.42	0.00	0.00	0.00	0.00	0.00	0.00E+00	0.00E+00	0.00E+00	2.61E+06	0.00E+00	1.10E+07	2.09E+06	0.00E+00
986.35	2.75	1.12	41.54	0.48	0.00	0.00	0.01	0.00	0.00	0.00E+00	0.00E+00	0.00E+00	4.18E+06	0.00E+00	3.86E+06	7.31E+05	0.00E+00
980.66	4.46	7.16	54.05	1.69	0.00	0.00	0.00	0.00	0.00	0.00E+00	0.00E+00	0.00E+00	1.36E+06	0.00E+00	4.49E+06	1.04E+06	0.00E+00
976.39	2.09	3.05	78.27	0.00	0.00	0.00	0.00	0.00	0.00	0.00E+00	0.00E+00	3.65E+06	1.83E+06	0.00E+00	5.74E+06	1.83E+06	0.00E+00
972.12	2.80	2.95	76.19	0.84	0.00	0.00	0.00	0.00	0.00	0.00E+00	0.00E+00	0.00E+00	8.35E+05	0.00E+00	7.62E+06	1.36E+06	0.00E+00
963.58	0.55	3.71	45.70	0.39	0.00	0.00	0.17	0.00	0.00	0.00E+00	0.00E+00	2.09E+06	5.22E+06	0.00E+00	9.92E+06	2.09E+04	0.00E+00
959.31	0.71	6.23	31.14	1.18	0.29	0.00	0.00	0.00	0.00	0.00E+00	0.00E+00	0.00E+00	2.09E+06	0.00E+00	1.25E+07	7.31E+05	0.00E+00
955.04	3.53	3.53	50.98	1.26	0.00	0.00	0.30	0.00	0.00	0.00E+00	0.00E+00	0.00E+00	2.40E+06	0.00E+00	1.39E+07	1.04E+06	0.00E+00
950.77	0.00	6.67	30.66	0.67	0.27	0.00	0.27	0.00	0.00	0.00E+00	0.00E+00	1.04E+06	4.18E+06	0.00E+00	1.10E+07	1.30E+06	0.00E+00
946.50	2.67	6.85	10.66	1.52	0.00	0.00	0.15	0.00	0.00	0.00E+00	0.00E+00	0.00E+00	2.09E+06	0.00E+00	1.20E+07	1.04E+06	3.13E+05
943.00	1.28	1.28	2.93	0.89	0.00	0.00	0.00	0.00	0.00	0.00E +00	0.00E+00	0.00E+00	1.30E+06	0.00E+00	4.18E+06	2.35E+06	0.00E+00
939.50	2.29	2.45	0.52	0.00	0.00	0.82	0.00	0.00	0.00	0.00E+00	0.00E+00	0.00E+00	1.83E+06	0.00E+00	2.09E+06	1.30E+06	0.00E+00
936.00	0.40	0.20	0.40	0.28	0.00	0.12	0.00	0.00	0.00	0.00E+00	0.00E+00	0.00E+00	1.04E+06	0.00E+00	2.61E+06	1.04E+06	0.00E+00
929.00	0.00	0.26	0.34	0.26	0.00	0.00	0.00	0.00	0.00	0.00E+00	0.00E+00	0.00E+00	1.36E+06	0.00E+00	1.77E+06	1.77E+06	0.00E+00
925.50	0.83	3.46	1.38	0.83	0.00	0.00	0.00	0.00	0.00	0.00E+00	0.00E+00	0.00E+00	6.47E+05	0.00E+00	1.77E+06	1.77E+06	0.00E+00
922.00	0.42	0.56	0.33	0.16	0.00	0.08	0.00	0.00	0.00	0.00E+00	0.00E+00	5.22E+05	2.82E+06	0.00E+00	1.04E+06	1.77E+06	0.00E+00
918.22	3.56	1.78	0.00	0.00	0.00	0.00	0.00	0.00	0.00	0.00E+00	0.00E+00	0.00E+00	2.09E+06	0.00E+00	4.91E+06	3.13E+06	0.00E+00
914.45	3.08	0.56	0.00	0.00	0.00	0.00	0.19	0.00	0.00	0.00E+00	0.00E+00	0.00E+00	3.86E+06	0.00E+00	5.22E+06	2.40E+06	0.00E+00
910.68	0.30	0.76	0.19	0.00	0.00	0.00	0.08	0.00	0.00	0.00E+00	0.00E+00	5.22E+05	5.22E+06	0.00E+00	8.87E+06	1.04E+06	0.00E+00
902.12	0.19	0.19	0.00	0.05	0.00	0.13	0.00	0.00	0.00	0.00E+00	0.00E+00	0.00E+00	4.70E+06	0.00E+00	2.09E+06	3.45E+06	0.00E+00
893.56	0.74	0.50	0.06	0.13	0.00	0.09	0.00	0.00	0.00	0.00E+00	0.00E+00	0.00E+00	5.22E+06	0.00E+00	3.65E+06	4.91E+06	0.00E+00
889.20	0.13	0.71	0.00	0.26	0.19	0.04	0.00	0.00	0.00	0.00E+00	0.00E+00	5.22E+05	1.57E+07	0.00E+00	3.65E+06	2.61E+06	0.00E+00
885.00	0.76	1.66	0.00	0.30	0.15	0.00	0.00	0.00	0.18	0.00E+00	0.00E+00	0.00E+00	7.31E+06	0.00E+00	1.30E+06	4.80E+06	0.00E+00
881.00	2.75	1.69	3.14	0.72	0.14	0.10	0.00	0.00	0.00	0.00E+00	0.00E+00	0.00E+00	6.79E+06	0.00E+00	4.70E+06	3.86E+06	0.00E+00
875.75	1.07	2.18	5.96	0.40	0.08	0.04	0.08	0.00	0.00	0.00E+00	0.00E+00	5.22E+05	3.65E+06	0.00E+00	4.49E+06	2.09E+06	0.00E+00
867.63	2.42	0.91	1.03	0.30	0.00	0.76	0.00	0.00	0.00	0.00E+00	0.00E+00	0.00E+00	4.18E+06	5.22E+05	2.61E+06	5.22E+06	0.00E+00
859.50	1.16	0.78	1.75	0.27	0.00	0.19	0.00	0.00	0.00	0.00E+00	0.00E+00	5.22E+05	3.13E+06	0.00E+00	4.91E+06	6.26E+06	0.00E+00
853.00	0.97	0.73	1.94	0.82	0.10	0.97	0.00	0.00	0.00	0.00E+00	0.00E+00	0.00E+00	2.82E+06	0.00E+00	4.91E+06	4.49E+06	0.00E+00
846.50	2.07	2.97	5.85	2.02	0.00	1.35	0.00	0.00	0.00	0.00E+00	0.00E+00	0.00E+00	2.40E+06	0.00E+00	4.70E+06	2.40E+06	0.00E+00
842.55	2.30	1.56	11.97	1.38	0.00	0.92	0.00	0.00	0.00	0.00E+00	0.00E+00	0.00E+00	3.65E+06	5.22E+05	4.18E+06	4.91E+06	0.00E+00
838.60	1.15	1.35	1.15	1.13	0.00	1.00	0.00	0.00	0.00	0.00E+00	0.00E+00	0.00E+00	2.61E+06	0.00E+00	3.65E+06	5.74E+06	0.00E+00
834.70	0.23	1.27	4.69	0.61	0.00	0.94	0.00	0.00	0.00	0.00E+00	0.00E+00	0.00E+00	4.70E+06	0.00E+00	7.31E+06	4.18E+06	0.00E+00
830.80	0.39	2.56	0.85	0.23	0.00	0.00	0.00	0.00	0.00	0.00E+00	0.00E+00	2.09E+06	4.18E+06	0.00E+00	5.22E+06	1.77E+06	0.00E+00
823.00	0.31	1.63	0.09	0.15	0.00	0.00	0.00	0.00	0.15	0.00E+00	0.00E+00	2.09E+06	6.79E+06	0.00E+00	1.04E+06	2.09E+06	0.00E+00
819.10	0.31	0.50	0.13	0.24	0.00	0.00	0.00	0.00	0.02	0.00E+00	0.00E+00	3.13E+06	2.09E+06	0.00E+00	2.09E+06	2.09E+06	0.00E+00
815.20	0.50	0.90	0.67	0.23	0.00	0.00	0.00	0.00	0.00	0.00E+00	0.00E+00	0.00E+00	3.13E+06	0.00E+00	1.04E+06	3.13E+06	0.00E+00
811.30	1.18	0.62	1.09	0.00	0.05	0.00	0.00	0.00	0.00	0.00E+00	0.00E+00	1.04E+06	5.74E+06	0.00E+00	2.09E+06	3.86E+06	0.00E+00
807.40	2.72	1.01	0.50	1.31	0.00	0.00	0.00	0.00	0.00	0.00E+00	0.00E+00	5.22E+05	4.18E+06	0.00E+00	3.65E+06	2.09E+06	0.00E+00
803.50	3.10	0.21	0.00	1.21	0.21	0.00	0.00	0.00	0.17	0.00E+00	0.00E+00	0.00E+00	4.91E+06	0.00E+00	4.18E+06	3.13E+06	0.00E+00
799.60	3.12	0.21	1.18	0.35	0.00	0.00	0.00	0.00	0.00	0.00E+00	0.00E+00	0.00E+00	7.31E+06	0.00E+00	2.09E+06	3.13E+06	0.00E+00
795.70	3.08	0.23	0.23	1.08	0.00	0.00	0.00	0.00	0.00	0.00E+00	0.00E+00	0.00E+00	5.74E+06	1.04E+06	2.61E+06	2.61E+06	0.00E+00
789.90	2.98	0.29	2.86	0.34	0.00	0.00	0.00	0.00	0.00	0.00E+00	0.00E+00	1.04E+06	5.95E+06	0.00E+00	2.40E+06	1.57E+06	0.00E+00
784.00	5.90	0.00	2.55	0.67	0.00	0.00	0.00	0.00	0.00	0.00E+00	0.00E+00	0.00E+00	3.86E+06	0.00E+00	2.61E+06	5.74E+06	0.00E+00
779.20	2.61	0.00	2.61	3.39	0.00	0.00	0.00	0.00	0.00	0.00E+00	0.00E+00	5.22E+05	3.86E+06	6.26E+05	2.82E+06	5.22E+05	0.00E+00
774.60	4.93	0.00	2.99	0.75	0.00	0.00	0.00	0.00	0.00	0.00E+00	0.00E+00	1.04E+06	6.26E+06	0.00E+00	3.13E+06	1.57E+06	0.00E+00

(continued on next page)

Appendix B (*continued*)

Depth (cm)	*Syracosphaera* (%)	*G. rotula* (%)	*G. jafari* (%)	*R. clavigera* (%)	*Calciosolenia* (%)	*R. rotaria* (%)	*L. perdurum* (%)	*H. macroporus* (%)	*Amaurolithus* (%)	*Reticulofenestra* <5/g	*Reticulofenestra* >5/g	*Dictyococcites* (/g)	*C. pelagicus* <10/g	*C. pelagicus* >10/g	*H. carteri* (/g)	*C. leptoporus* (/g)	*C. macintyrei* (/g)
768.40	4.51	0.00	12.03	2.63	0.00	0.00	0.00	0.00	0.00	0.00E+00	0.00E+00	0.00E+00	5.22E+06	5.22E+05	1.04E+06	4.18E+06	0.00E+00
765.20	7.88	0.15	8.75	6.56	0.00	0.00	0.00	0.00	0.00	0.00E+00	0.00E+00	5.22E+05	6.26E+06	0.00E+00	1.04E+06	1.36E+06	0.00E+00
760.60	4.95	1.39	3.37	0.99	0.00	0.00	0.00	0.00	0.00	0.00E+00	0.00E+00	5.22E+05	5.74E+06	0.00E+00	2.09E+06	3.65E+06	0.00E+00
756.00	5.17	0.00	33.12	1.03	0.26	0.31	0.00	0.00	0.00	0.00E+00	0.00E+00	0.00E+00	2.09E+06	0.00E+00	1.77E+06	5.22E+06	0.00E+00
749.50	4.32	0.00	5.76	0.58	0.96	0.00	0.00	0.00	0.00	0.00E+00	0.00E+00	1.57E+06	8.87E+06	5.22E+05	1.36E+06	1.04E+06	0.00E+00
746.25	4.21	0.00	2.81	2.11	0.42	0.01	0.18	0.00	0.00	0.00E+00	0.00E+00	0.00E+00	8.35E+06	0.00E+00	1.04E+06	2.40E+06	0.00E+00
743.00	8.29	0.00	2.91	0.90	0.00	0.00	0.00	0.22	0.00	0.00E+00	0.00E+00	1.57E+06	5.95E+06	0.00E+00	1.57E+06	7.83E+05	0.00E+00
739.75	4.38	0.44	0.73	1.90	0.00	0.00	0.15	0.00	0.00	0.00E+00	0.00E+00	5.22E+05	3.13E+06	0.00E+00	3.13E+06	1.25E+06	0.00E+00
736.50	4.64	1.83	1.41	0.70	0.00	0.00	0.00	0.00	0.00	0.00E+00	0.00E+00	0.00E+00	5.22E+06	0.00E+00	8.87E+06	1.57E+06	0.00E+00
733.25	10.75	1.96	0.49	0.39	0.78	0.00	0.00	0.20	0.00	0.00E+00	0.00E+00	0.00E+00	5.22E+06	0.00E+00	8.04E+06	7.83E+05	0.00E+00
729.13	3.38	0.51	0.00	0.51	0.00	0.00	0.06	0.05	0.00	0.00E+00	0.00E+00	0.00E+00	8.35E+06	0.00E+00	2.04E+07	1.04E+06	0.00E+00
725.00	2.62	0.73	0.00	1.05	0.31	0.00	0.00	0.00	0.00	0.00E+00	0.00E+00	0.00E+00	7.83E+06	0.00E+00	1.67E+07	0.00E+00	0.00E+00
720.00	1.51	1.51	0.00	0.89	0.00	0.00	0.00	0.00	0.00	0.00E+00	0.00E+00	5.22E+05	8.87E+06	5.22E+05	9.92E+06	1.30E+06	0.00E+00
715.00	2.52	0.55	0.00	1.09	0.00	0.00	0.05	0.00	0.00	0.00E+00	0.00E+00	0.00E+00	6.99E+06	0.00E+00	7.31E+06	1.77E+06	0.00E+00
710.00	2.15	0.30	0.30	2.86	0.54	0.00	0.00	0.00	0.00	0.00E+00	0.00E+00	0.00E+00	4.91E+06	0.00E+00	2.09E+06	1.04E+06	0.00E+00
705.00	2.03	0.36	0.00	1.19	0.00	0.36	0.00	0.00	0.00	0.00E+00	0.00E+00	5.22E+05	3.86E+06	0.00E+00	2.09E+06	1.57E+06	0.00E+00
700.91	0.59	0.00	0.24	0.00	0.55	0.00	0.00	0.00	0.00	0.00E+00	0.00E+00	0.00E+00	9.40E+06	0.00E+00	3.45E+06	1.04E+06	0.00E+00
696.78	1.42	0.25	1.06	0.25	0.00	0.09	0.00	0.00	0.00	0.00E+00	0.00E+00	0.00E+00	5.74E+06	0.00E+00	7.31E+06	3.86E+06	0.00E+00
688.52	0.44	0.66	0.00	0.07	0.07	0.00	0.00	0.07	0.00	0.00E+00	0.00E+00	0.00E+00	9.92E+06	0.00E+00	6.79E+06	8.98E+06	0.00E+00
684.39	0.69	0.31	0.31	0.20	0.11	0.00	0.00	0.00	0.00	0.00E+00	0.00E+00	0.00E+00	9.40E+06	0.00E+00	3.13E+06	4.18E+06	0.00E+00
680.26	0.52	0.21	0.48	0.10	0.06	0.14	0.00	0.00	0.00	0.00E+00	0.00E+00	0.00E+00	6.79E+06	0.00E+00	7.83E+06	2.09E+06	0.00E+00
676.13	0.35	0.46	0.25	0.25	0.11	0.11	0.00	0.00	0.00	0.00E+00	0.00E+00	5.22E+05	6.58E+06	0.00E+00	4.49E+06	6.58E+06	0.00E+00
672.00	0.16	0.32	0.32	0.25	0.00	0.00	0.00	0.05	0.00	0.00E+00	0.00E+00	0.00E+00	1.04E+06	0.00E+00	1.04E+06	4.18E+06	0.00E+00
668.50	1.12	0.61	0.00	0.62	0.52	0.34	0.00	0.00	0.01	0.00E+00	0.00E+00	5.22E+05	4.18E+06	0.00E+00	3.13E+06	3.13E+06	0.00E+00
664.75	1.94	3.37	0.93	2.37	0.36	1.97	0.00	0.07	0.04	0.00E+00	0.00E+00	0.00E+00	3.86E+06	0.00E+00	3.86E+06	9.40E+06	0.00E+00
661.00	1.55	0.93	2.56	1.32	0.23	1.24	0.00	0.00	0.00	0.00E+00	0.00E+00	1.57E+06	2.09E+06	0.00E+00	2.09E+06	8.66E+06	0.00E+00
651.26	1.96	4.26	2.30	2.01	0.00	0.00	0.00	0.00	0.00	0.00E+00	0.00E+00	0.00E+00	1.04E+06	2.61E+05	2.40E+06	3.13E+06	0.00E+00
646.40	0.38	1.92	0.96	1.31	0.00	0.00	0.00	0.00	0.08	0.00E+00	0.00E+00	2.09E+06	2.09E+06	0.00E+00	1.04E+06	3.13E+06	0.00E+00
642.78	0.99	1.82	2.13	1.58	0.40	0.00	0.00	0.00	0.00	0.00E+00	0.00E+00	5.22E+05	1.77E+06	0.00E+00	7.31E+05	1.04E+06	0.00E+00
639.16	2.38	1.43	0.95	0.57	0.00	0.00	0.00	0.00	0.00	0.00E+00	0.00E+00	0.00E+00	6.26E+06	0.00E+00	1.83E+06	6.37E+06	0.00E+00
635.54	0.31	2.02	0.37	0.00	0.61	0.00	0.00	0.00	0.06	0.00E+00	0.00E+00	2.61E+06	5.22E+05	5.22E+05	0.00E+00	7.31E+05	0.00E+00
631.92	1.78	1.36	0.00	0.77	0.18	0.00	0.00	0.00	0.09	0.00E+00	0.00E+00	0.00E+00	4.18E+06	0.00E+00	0.00E+00	4.70E+06	0.00E+00
628.30	5.59	2.24	1.45	1.12	0.00	0.00	0.22	0.00	0.00	0.00E+00	0.00E+00	0.00E+00	3.13E+06	0.00E+00	5.22E+05	3.13E+06	7.31E+05
624.68	1.08	1.27	0.95	0.32	0.00	0.64	0.00	0.19	0.00	0.00E+00	0.00E+00	2.61E+06	1.57E+06	0.00E+00	1.04E+06	2.09E+06	0.00E+00
617.44	0.80	3.19	0.80	0.40	0.40	0.00	0.00	0.00	0.00	0.00E+00	0.00E+00	5.22E+05	2.61E+06	0.00E+00	2.09E+06	3.13E+05	0.00E+00
613.82	0.42	1.26	0.84	1.93	0.13	0.00	0.00	0.00	0.00	0.00E+00	0.00E+00	0.00E+00	1.57E+06	0.00E+00	2.61E+06	5.22E+05	0.00E+00
610.20	2.54	2.97	0.21	0.13	0.13	0.13	0.00	0.00	0.00	0.00E+00	0.00E+00	1.04E+06	2.92E+06	0.00E+00	1.04E+06	6.26E+05	0.00E+00
606.58	0.76	2.06	0.00	0.08	0.00	0.00	0.00	0.00	0.08	0.00E+00	0.00E+00	2.09E+06	2.40E+06	0.00E+00	1.83E+06	7.31E+05	0.00E+00
602.96	1.48	1.48	0.00	0.30	0.00	0.30	0.00	0.00	0.00	0.00E+00	0.00E+00	0.00E+00	2.61E+06	0.00E+00	2.09E+06	3.65E+06	0.00E+00
599.34	1.58	0.89	1.37	0.89	0.69	0.00	0.00	0.00	0.07	0.00E+00	0.00E+00	2.09E+06	4.18E+06	0.00E+00	3.13E+06	2.61E+06	0.00E+00
595.72	1.77	1.47	8.84	1.13	1.82	0.00	0.00	0.00	0.00	0.00E+00	0.00E+00	5.22E+05	4.70E+06	0.00E+00	1.51E+07	1.77E+06	0.00E+00
592.10	2.48	0.62	6.19	0.93	0.93	0.00	0.00	0.00	0.00	0.00E+00	0.00E+00	5.22E+05	4.70E+06	0.00E+00	8.87E+06	5.22E+06	0.00E+00
584.86	1.21	2.01	0.28	0.00	0.00	0.00	0.00	0.00	0.00	0.00E+00	0.00E+00	0.00E+00	7.31E+06	0.00E+00	4.18E+06	1.10E+07	0.00E+00
581.24	1.23	2.58	0.00	0.20	0.41	0.41	0.00	0.00	0.00	0.00E+00	0.00E+00	5.22E+05	1.36E+07	0.00E+00	1.10E+07	8.87E+06	0.00E+00
577.62	1.98	6.46	0.00	1.21	0.42	0.00	0.00	0.00	0.00	0.00E+00	0.00E+00	1.04E+06	7.83E+06	0.00E+00	8.35E+06	1.10E+07	5.22E+05
574.00	0.85	1.58	0.26	0.48	0.48	0.00	0.04	0.11	0.09	0.00E+00	0.00E+00	0.00E+00	5.74E+06	0.00E+00	9.92E+06	8.35E+06	0.00E+00
570.10	1.27	2.14	0.00	0.14	0.71	0.00	0.08	0.06	0.00	0.00E+00	0.00E+00	5.22E+05	1.15E+07	0.00E+00	3.13E+06	8.35E+06	0.00E+00

566.20	4.10	2.74	0.00	0.60	0.09	0.00	0.00	0.17	0.00	0.00E+00	0.00E+00	5.22E+05	6.26E+06	0.00E+00	5.74E+06	1.10E+07	0.00E+00
562.38	1.34	2.97	0.00	0.53	0.81	0.00	0.04	0.00	0.00	0.00E+00	0.00E+00	0.00E+00	8.35E+06	0.00E+00	7.83E+06	1.25E+07	0.00E+00
558.56	1.01	4.21	4.21	0.36	0.36	0.00	0.00	0.00	0.00	0.00E+00	0.00E+00	1.57E+06	8.35E+06	0.00E+00	5.85E+06	7.31E+06	0.00E+00
550.92	0.96	4.78	0.38	0.50	0.38	0.00	0.00	0.00	0.00	0.00E+00	0.00E+00	5.22E+05	8.87E+06	0.00E+00	3.65E+06	7.31E+06	0.00E+00
547.10	2.03	6.67	0.00	0.93	1.01	0.00	0.06	0.00	0.00	0.00E+00	0.00E+00	0.00E+00	1.10E+07	0.00E+00	6.79E+06	1.11E+07	0.00E+00
543.28	3.07	5.37	0.00	0.54	1.53	0.00	0.00	0.00	0.00	0.00E+00	0.00E+00	5.22E+05	1.00E+07	0.00E+00	6.58E+06	7.52E+06	0.00E+00
539.46	0.60	4.93	0.20	0.20	0.26	0.00	0.00	0.00	0.00	0.00E+00	0.00E+00	1.57E+06	7.31E+06	0.00E+00	6.79E+06	4.70E+07	0.00E+00
535.64	2.97	32.71	0.00	1.59	0.30	0.00	0.10	0.00	0.00	0.00E+00	0.00E+00	0.00E+00	6.26E+06	0.00E+00	1.41E+07	4.18E+06	0.00E+00
531.82	8.97	16.44	0.00	1.12	1.49	0.00	0.15	0.00	0.00	0.00E+00	0.00E+00	5.22E+05	7.31E+06	0.00E+00	1.98E+07	2.09E+06	0.00E+00
528.21	6.98	16.41	0.91	0.87	0.00	0.00	0.00	0.00	0.00	0.00E+00	0.00E+00	1.04E+06	2.51E+07	0.00E+00	2.61E+07	0.00E+00	0.00E+00
524.61	7.65	4.85	7.06	0.43	0.00	0.00	0.68	0.51	0.00	0.00E+00	0.00E+00	0.00E+00	3.65E+07	0.00E+00	1.25E+07	2.82E+06	0.00E+00
521.00	4.89	1.51	3.56	0.53	0.44	0.00	0.00	0.44	0.00	0.00E+00	0.00E+00	5.22E+05	1.46E+07	0.00E+00	1.98E+07	1.57E+06	0.00E+00
515.00	5.65	2.13	16.69	0.00	1.25	0.00	0.00	0.00	0.00	0.00E+00	0.00E+00	0.00E+00	9.92E+06	0.00E+00	2.40E+07	2.09E+06	0.00E+00
509.00	1.96	0.65	4.25	0.00	0.00	0.00	0.00	0.00	0.65	0.00E+00	0.00E+00	5.22E+05	1.46E+07	0.00E+00	2.04E+07	1.25E+06	0.00E+00
503.00	1.05	0.25	3.86	0.35	0.00	0.18	0.00	0.04	0.00	0.00E+00	0.00E+00	3.13E+06	0.00E+00	1.25E+07	1.30E+07	5.22E+06	2.09E+06
497.00	0.53	0.69	4.24	0.53	0.53	0.16	0.00	0.05	0.26	0.00E+00	0.00E+00	5.22E+05	1.57E+07	0.00E+00	1.77E+07	4.18E+06	0.00E+00
491.00	1.42	0.62	1.05	0.19	0.19	0.00	0.00	0.00	0.00	0.00E+00	0.00E+00	0.00E+00	8.87E+06	0.00E+00	9.92E+06	4.18E+06	0.00E+00
485.00	0.66	0.75	1.33	0.22	0.00	0.44	0.00	0.00	0.00	0.00E+00	0.00E+00	5.22E+05	8.87E+06	0.00E+00	4.70E+06	3.65E+06	0.00E+00
480.50	0.74	0.25	0.31	0.12	0.05	0.07	0.00	0.00	0.00	0.00E+00	0.00E+00	5.22E+05	1.41E+07	0.00E+00	8.35E+06	4.91E+06	0.00E+00
476.00	0.08	0.16	1.03	0.16	0.00	0.16	0.00	0.00	0.00	0.00E+00	0.00E+00	1.04E+06	1.04E+06	0.00E+00	2.82E+06	4.70E+06	0.00E+00
467.00	1.27	0.60	0.11	0.46	0.18	0.88	0.00	0.00	0.00	0.00E+00	0.00E+00	0.00E+00	7.31E+06	0.00E+00	5.22E+06	6.79E+06	5.22E+05
462.50	1.17	1.58	1.00	2.17	1.17	1.76	0.00	0.00	0.00	0.00E+00	0.00E+00	0.00E+00	3.45E+06	0.00E+00	3.65E+06	8.35E+06	0.00E+00
458.00	9.35	3.55	1.08	5.38	5.05	1.08	0.00	0.00	0.00	0.00E+00	0.00E+00	0.00E+00	1.57E+06	5.22E+05	4.70E+06	9.92E+06	0.00E+00
453.00	2.27	2.40	0.00	1.94	0.97	0.00	0.06	0.00	0.00	0.00E+00	0.00E+00	0.00E+00	8.87E+06	0.00E+00	6.26E+06	8.35E+06	1.04E+06
448.00	2.32	5.73	0.00	3.10	2.32	0.77	0.00	0.00	0.00	0.00E+00	0.00E+00	5.22E+05	2.09E+06	0.00E+00	1.04E+06	2.82E+06	0.00E+00
443.00	6.24	3.18	0.82	6.24	5.88	0.00	0.00	0.00	0.71	0.00E+00	0.00E+00	0.00E+00	1.57E+06	0.00E+00	1.04E+07	6.26E+06	0.00E+00
438.00	2.00	2.30	0.30	3.70	2.70	0.00	0.00	0.00	0.50	0.00E+00	0.00E+00	0.00E+00	3.65E+06	0.00E+00	6.79E+06	5.95E+06	0.00E+00
428.00	2.19	2.74	0.00	1.81	5.10	0.00	0.00	0.00	0.16	0.00E+00	0.00E+00	0.00E+00	3.13E+05	0.00E+00	1.01E+07	7.31E+06	0.00E+00
421.90	6.51	2.21	1.30	1.95	7.17	0.00	0.00	0.00	0.00	0.00E+00	0.00E+00	0.00E+00	3.13E+06	0.00E+00	5.95E+06	7.62E+06	0.00E+00
415.80	1.71	3.68	0.00	1.11	2.78	0.00	0.00	0.00	0.00	0.00E+00	0.00E+00	0.00E+00	1.77E+06	0.00E+00	2.09E+06	9.92E+06	0.00E+00
409.70	2.21	2.21	0.00	0.20	2.01	0.00	0.00	0.00	0.00	0.00E+00	0.00E+00	0.00E+00	5.22E+05	0.00E+00	3.65E+06	7.31E+06	0.00E+00
405.12	0.68	1.61	0.00	1.09	1.49	1.21	0.00	0.00	0.00	0.00E+00	0.00E+00	0.00E+00	5.22E+05	0.00E+00	2.61E+06	1.72E+07	0.00E+00
400.54	0.37	2.23	0.45	1.49	0.97	0.00	0.00	0.00	0.00	0.00E+00	0.00E+00	0.00E+00	7.31E+05	0.00E+00	6.99E+06	4.91E+06	0.00E+00
395.96	1.44	1.88	0.00	1.88	4.20	0.19	0.00	0.00	0.00	0.00E+00	0.00E+00	3.13E+05	2.40E+06	0.00E+00	1.77E+06	4.49E+06	0.00E+00
391.38	1.14	1.78	2.63	1.21	3.56	0.00	0.00	0.00	0.00	0.00E+00	0.00E+00	1.57E+06	2.61E+06	0.00E+00	4.70E+06	5.85E+06	0.00E+00
386.80	3.65	2.43	2.19	1.62	1.22	0.00	0.00	0.00	0.00	0.00E+00	0.00E+00	2.09E+06	3.65E+06	0.00E+00	3.13E+06	1.36E+06	1.04E+06
377.64	3.83	0.46	13.98	7.29	1.22	0.00	0.00	0.00	0.00	0.00E+00	0.00E+00	5.22E+05	3.13E+06	0.00E+00	3.13E+06	4.18E+06	0.00E+00
373.06	1.13	1.30	4.52	1.13	0.00	0.28	0.00	0.00	0.00	0.00E+00	0.00E+00	1.57E+06	4.70E+06	0.00E+00	3.13E+06	4.70E+06	0.00E+00
368.48	1.11	0.21	2.57	0.90	0.00	0.35	0.00	0.00	0.00	0.00E+00	0.00E+00	0.00E+00	2.61E+06	0.00E+00	5.22E+06	1.57E+06	0.00E+00
363.90	0.93	0.82	0.58	0.33	0.33	0.00	0.00	0.00	0.00	0.00E+00	0.00E+00	7.31E+05	3.65E+06	0.00E+00	5.22E+05	1.57E+06	0.00E+00
359.32	0.49	0.68	0.89	0.59	0.30	0.00	0.00	0.00	0.00	0.00E+00	0.00E+00	1.57E+06	5.22E+05	0.00E+00	2.61E+06	1.36E+06	0.00E+00
354.74	1.30	0.80	1.65	1.50	0.50	0.00	0.00	0.00	0.00	0.00E+00	0.00E+00	0.00E+00	6.26E+06	0.00E+00	1.04E+06	1.57E+06	0.00E+00
349.31	3.33	0.33	3.00	1.11	0.33	0.00	0.00	0.00	0.44	0.00E+00	0.00E+00	0.00E+00	1.04E+06	0.00E+00	7.83E+06	3.13E+06	0.00E+00
343.88	1.26	0.00	19.25	0.67	0.25	0.00	0.00	0.00	0.00	0.00E+00	0.00E+00	5.22E+05	5.22E+06	0.00E+00	5.85E+06	5.22E+06	5.22E+05
333.03	3.27	0.00	25.45	1.09	0.58	0.36	0.00	0.00	0.00	0.00E+00	0.00E+00	1.04E+06	3.13E+06	0.00E+00	1.04E+06	1.30E+06	0.00E+00
327.60	0.45	0.00	1.03	0.31	0.18	0.00	0.00	0.00	0.02	0.00E+00	0.00E+00	0.00E+00	1.77E+06	0.00E+00	1.30E+06	2.71E+06	0.00E+00
321.00	0.66	0.00	1.00	0.17	0.33	0.00	0.02	0.00	0.00	0.00E+00	0.00E+00	0.00E+00	7.62E+06	0.00E+00	2.40E+06	4.49E+06	0.00E+00
317.55	1.89	0.00	16.54	0.24	0.00	0.00	0.24	0.00	0.00	0.00E+00	0.00E+00	5.22E+05	7.31E+06	5.22E+05	1.77E+06	1.36E+06	0.00E+00
314.10	4.00	0.06	5.22	2.06	0.00	0.00	0.00	0.00	0.00	0.00E+00	0.00E+00	0.00E+00	9.40E+06	0.00E+00	1.04E+06	2.40E+06	0.00E+00
310.65	6.93	0.00	15.31	0.00	0.00	0.00	0.00	0.00	0.00	0.00E+00	0.00E+00	0.00E+00	5.22E+06	0.00E+00	5.22E+06	4.18E+06	5.22E+05

(continued on next page)

Appendix B (*continued*)

Depth (cm)	*Syracosphaera* (%)	*G. rotula* (%)	*G. jafari* (%)	*R. clavigera* (%)	*Calciosolenia* (%)	*R. rotaria* (%)	*L. perdurum* (%)	*H. macroporus* (%)	*Amaurolithus* (%)	*Reticulofenestra* <5/g	*Reticulofenestra* >5/g	*Dictyococcites* (/g)	*C. pelagicus* <10/g	*C. pelagicus* >10/g	*H. carteri* (/g)	*C. leptoporus* (/g)	*C. macintyrei* (/g)
307.20	3.57	0.33	22.45	1.58	0.26	0.00	0.00	0.00	0.00	0.00E+00	0.00E+00	2.09E+06	7.83E+06	5.22E+05	3.13E+06	7.31E+06	3.13E+05
298.60	3.66	0.00	15.39	1.95	1.71	0.00	0.00	0.00	0.00	0.00E+00	0.00E+00	5.22E+05	2.09E+05	0.00E+00	1.36E+06	4.18E+06	0.00E+00
290.00	3.61	1.56	28.88	2.77	0.60	0.60	0.00	0.00	0.00	0.00E+00	0.00E+00	3.13E+05	4.91E+06	0.00E+00	3.45E+06	5.22E+06	0.00E+00
285.25	56.89	0.00	0.00	0.00	0.00	0.00	0.00	0.00	0.00	0.00E+00	0.00E+00	1.57E+06	3.45E+06	0.00E+00	1.77E+06	2.82E+06	0.00E+00
280.50	2.95	0.44	40.57	1.48	0.37	0.00	0.00	0.00	0.00	0.00E+00	0.00E+00	0.00E+00	4.18E+06	0.00E+00	1.36E+06	2.82E+06	0.00E+00
274.66	2.88	2.88	36.66	1.44	0.00	0.00	0.00	0.00	0.00	0.00E+00	0.00E+00	0.00E+00	3.86E+06	0.00E+00	2.09E+06	4.18E+06	0.00E+00
268.83	2.59	0.78	21.76	0.62	1.04	0.00	0.00	0.00	0.00	0.00E+00	0.00E+00	1.57E+06	3.13E+06	0.00E+00	5.53E+06	2.09E+06	0.00E+00
263.00	1.23	7.03	6.50	4.04	0.00	0.00	0.00	0.00	0.00	0.00E+00	0.00E+00	5.22E+05	5.22E+06	0.00E+00	3.13E+06	0.00E+00	0.00E+00
253.00	2.17	0.89	2.55	0.00	0.77	0.00	0.00	0.00	0.00	0.00E+00	0.00E+00	1.04E+06	3.65E+06	0.00E+00	3.13E+06	1.04E+06	0.00E+00
241.00	1.90	0.00	1.90	0.00	0.00	0.00	0.00	0.00	0.00	0.00E+00	0.00E+00	0.00E+00	4.18E+06	0.00E+00	1.57E+06	5.22E+05	0.00E+00
235.20	1.80	1.35	0.90	0.36	0.00	0.00	0.00	0.18	0.00	0.00E+00	0.00E+00	0.00E+00	2.09E+06	0.00E+00	1.57E+06	0.00E+00	0.00E+00
223.60	0.01	0.27	0.11	0.11	0.00	0.11	0.00	0.00	0.00	0.00E+00	0.00E+00	1.04E+05	4.18E+06	0.00E+00	2.09E+06	1.04E+06	0.00E+00
219.73	0.00	0.13	0.00	0.00	0.00	0.00	0.00	0.00	0.00	0.00E+00	0.00E+00	5.22E+05	2.82E+06	0.00E+00	3.13E+05	0.00E+00	0.00E+00
212.00	0.18	0.14	0.00	0.32	0.14	0.23	0.00	0.00	0.00	0.00E+00	0.00E+00	5.22E+05	5.74E+06	0.00E+00	5.22E+05	6.26E+05	0.00E+00
204.00	0.14	0.42	0.04	0.07	0.00	0.04	0.00	0.00	0.00	0.00E+00	0.00E+00	1.57E+06	7.83E+06	0.00E+00	2.09E+06	2.09E+06	0.00E+00
196.00	0.22	0.34	0.08	0.05	0.17	0.09	0.03	0.00	0.00	0.00E+00	0.00E+00	5.22E+05	1.15E+07	0.00E+00	1.77E+06	3.13E+06	0.00E+00
180.00	0.45	0.90	0.00	0.52	0.11	0.29	0.00	0.00	0.02	0.00E+00	0.00E+00	5.22E+05	3.13E+06	0.00E+00	3.65E+06	1.77E+06	0.00E+00
172.00	0.64	1.54	0.28	0.92	0.36	0.98	0.00	0.00	0.00	0.00E+00	0.00E+00	1.57E+06	1.04E+06	5.22E+05	3.13E+06	3.65E+06	0.00E+00
156.00	0.64	1.58	0.12	0.40	0.40	0.47	0.00	0.00	0.00	0.00E+00	0.00E+00	0.00E+00	6.26E+05	0.00E+00	6.26E+05	1.04E+06	0.00E+00
150.33	1.11	2.44	0.33	1.00	0.10	0.90	0.00	0.00	0.00	0.00E+00	0.00E+00	1.04E+06	3.13E+06	0.00E+00	3.13E+06	4.70E+06	1.04E+06
139.00	0.98	1.85	0.84	0.98	0.84	0.86	0.00	0.00	0.05	0.00E+00	0.00E+00	5.22E+05	5.22E+05	0.00E+00	1.57E+06	1.57E+06	0.00E+00
128.50	0.76	1.71	0.19	0.28	0.00	1.71	0.04	0.00	0.00	0.00E+00	0.00E+00	7.31E+05	3.45E+06	0.00E+00	2.09E+06	2.09E+06	0.00E+00
123.25	2.14	0.56	0.13	0.43	0.11	0.00	0.00	0.00	0.00	0.00E+00	0.00E+00	1.57E+06	1.57E+06	0.00E+00	1.57E+06	1.04E+06	0.00E+00
112.75	0.73	0.65	0.31	0.36	0.00	0.00	0.02	0.00	0.02	0.00E+00	0.00E+00	0.00E+00	3.13E+06	0.00E+00	3.13E+06	2.09E+06	0.00E+00
107.50	1.20	0.80	0.00	1.20	0.00	0.00	0.00	0.00	0.00	0.00E+00	0.00E+00	1.04E+06	1.04E+06	5.22E+05	5.22E+05	2.61E+05	0.00E+00
103.75	0.38	0.77	0.15	0.80	0.15	0.00	0.00	0.00	0.00	0.00E+00	0.00E+00	5.22E+05	2.09E+06	0.00E+00	4.18E+06	5.22E+05	0.00E+00
100.00	3.38	0.36	2.71	0.51	0.51	0.00	0.00	0.00	0.00	0.00E+00	0.00E+00	0.00E+00	2.09E+06	0.00E+00	2.09E+06	7.83E+05	0.00E+00
92.50	0.98	0.46	0.11	0.28	0.37	0.00	0.00	0.00	0.00	0.00E+00	0.00E+00	4.18E+06	2.30E+06	2.61E+06	4.18E+06	1.83E+06	0.00E+00
88.75	2.55	1.32	0.00	1.78	0.00	0.00	0.00	0.00	0.00	0.00E+00	0.00E+00	0.00E+00	4.70E+06	5.22E+05	6.26E+06	7.31E+06	0.00E+00
81.25	2.72	0.17	0.19	1.18	0.08	0.00	0.00	0.00	0.00	0.00E+00	0.00E+00	4.70E+06	2.09E+06	0.00E+00	2.09E+06	1.77E+06	0.00E+00
65.50	2.48	0.54	0.00	0.32	0.43	0.00	0.00	0.00	0.00	0.00E+00	0.00E+00	1.04E+06	4.70E+06	0.00E+00	3.13E+06	5.22E+06	0.00E+00
60.50	5.42	1.58	0.45	0.18	0.27	0.00	0.00	0.00	0.00	0.00E+00	0.00E+00	1.57E+06	2.09E+06	0.00E+00	4.18E+06	3.13E+05	0.00E+00

Appendix B (*continued*)

Depth (cm)	*Sphenolithus* (/g)	*D. variabilis* (/g)	*D. pentaradiatus* (/g)	*D. brouweri* (/g)	*Pontosphaera* (/g)	*Syracosphaera* (/g)	*G. rotula* (/g)	*G. jafari* (/g)	*R. clavigera* (/g)	*Calciosolenia* (/g)	*R. rotaria* (/g)	*L. perdurum* (/g)	*H. macroporus* (/g)	*Amaurolithus* (/g)	TOTAL (liths/g)
992.04	1.04E+06	1.04E+06	0.00E+00	5.74E+06	7.31E+05	4.44E+06	1.30E+06	5.32E+07	6.26E+05	0.00E+00	0.00E+00	0.00E+00	0.00E+00	0.00E+00	1.50E+08
986.35	1.77E+06	1.04E+06	5.22E+04	4.70E+06	0.00E+00	4.49E+06	1.83E+06	6.79E+07	7.83E+05	0.00E+00	0.00E+00	1.04E+04	0.00E+00	0.00E+00	1.63E+08
980.66	1.04E+06	5.22E+04	0.00E+00	5.85E+06	1.36E+06	3.45E+06	5.53E+06	4.18E+07	1.30E+06	0.00E+00	0.00E+00	0.00E+00	0.00E+00	0.00E+00	7.73E+07
976.39	2.09E+06	7.83E+05	0.00E+00	4.96E+06	1.83E+06	5.22E+06	7.62E+06	1.96E+08	0.00E+00	0.00E+00	0.00E+00	0.00E+00	0.00E+00	0.00E+00	2.50E+08
972.12	4.18E+05	1.67E+05	0.00E+00	3.42E+06	3.45E+06	5.95E+06	6.26E+06	1.62E+08	1.77E+06	0.00E+00	0.00E+00	0.00E+00	0.00E+00	0.00E+00	2.12E+08
963.58	1.04E+06	1.04E+04	0.00E+00	1.04E+05	3.86E+06	1.04E+06	6.99E+06	8.61E+07	7.31E+05	0.00E+00	0.00E+00	3.13E+05	0.00E+00	0.00E+00	1.88E+08
959.31	0.00E+00	5.22E+05	0.00E+00	7.83E+05	3.13E+06	6.26E+05	5.53E+06	2.77E+07	1.04E+06	2.61E+05	0.00E+00	0.00E+00	0.00E+00	0.00E+00	8.88E+07
955.04	5.22E+05	3.13E+05	0.00E+00	6.26E+05	3.65E+06	3.65E+06	3.65E+06	5.27E+07	1.30E+06	0.00E+00	0.00E+00	3.13E+05	0.00E+00	0.00E+00	1.03E+08
950.77	5.22E+04	6.26E+04	0.00E+00	2.61E+05	3.13E+06	0.00E+00	5.22E+06	2.40E+07	5.22E+05	2.09E+05	0.00E+00	2.09E+05	0.00E+00	0.00E+00	7.83E+07
946.50	1.36E+06	3.13E+05	0.00E+00	1.67E+05	3.91E+06	1.83E+06	4.70E+06	7.31E+06	1.04E+06	0.00E+00	0.00E+00	1.04E +05	0.00E +00	0.00E +00	6.85E +07
943.00	3.13E+05	1.04E+06	0.00E+00	3.13E+05	2.92E+05	1.04E+06	1.04E+06	2.40E+06	7.31E+05	0.00E+00	0.00E+00	0.00E+00	0.00E+00	0.00E+00	8.18E+07
939.50	1.46E+05	0.00E+00	0.00E+00	0.00E+00	5.22E+05	7.31E+05	7.83E+05	1.67E+05	0.00E+00	0.00E+00	2.61E+05	0.00E+00	0.00E+00	0.00E+00	3.19E+07
936.00	3.13E+05	1.46E+05	0.00E+00	0.00E+00	2.61E+05	1.04E+06	5.22E+05	1.04E+06	7.31E+05	0.00E+00	3.13E+05	0.00E+00	0.00E+00	0.00E+00	2.59E+08
929.00	1.04E+06	1.67E+05	0.00E+00	5.22E+05	6.47E+05	0.00E+00	1.04E+06	1.36E+06	1.04E+06	0.00E+00	0.00E+00	0.00E+00	0.00E+00	0.00E+00	4.03E+08
925.50	5.95E+05	0.00E+00	0.00E+00	0.00E+00	2.30E+05	3.13E+05	1.30E+06	5.22E+05	3.13E+05	0.00E+00	0.00E+00	0.00E+00	0.00E+00	0.00E+00	3.77E+07
922.00	2.09E+05	2.30E+05	0.00E+00	0.00E+00	5.22E+05	1.36E+06	1.77E+06	1.04E+06	5.22E+05	0.00E+00	2.61E+05	0.00E+00	0.00E+00	0.00E+00	3.20E+08
918.22	0.00E+00	2.09E+05	0.00E+00	0.00E+00	0.00E+00	1.57E+06	7.83E+05	0.00E+00	0.00E+00	0.00E+00	0.00E+00	0.00E+00	0.00E+00	0.00E+00	4.40E+07
914.45	0.00E+00	5.95E+05	0.00E+00	2.92E+05	0.00E+00	1.73E+06	3.13E+05	0.00E+00	0.00E+00	0.00E+00	0.00E+00	1.04E+05	0.00E+00	0.00E+00	5.63E+07
910.68	0.00E+00	1.04E+06	0.00E+00	2.30E+05	5.22E+05	4.18E+05	1.04E+06	2.61E+05	0.00E+00	0.00E+00	0.00E+00	1.04E+05	0.00E+00	0.00E+00	1.38E+08
902.12	2.40E+06	7.41E+05	0.00E+00	0.00E+00	3.13E+05	1.04E+06	1.04E+06	0.00E+00	2.61E+05	0.00E+00	7.31E+05	0.00E+00	0.00E+00	0.00E+00	5.53E+08
893.56	1.04E+06	7.31E+05	0.00E+00	5.22E+05	1.67E+06	4.18E+06	2.82E+06	3.13E+05	7.31E+05	0.00E+00	5.22E+05	0.00E+00	0.00E+00	0.00E+00	5.68E+08
889.20	3.86E+06	2.09E+06	0.00E+00	0.00E+00	8.35E+05	1.04E+06	5.74E+06	0.00E+00	2.09E+06	1.57E+06	3.13E+05	0.00E+00	0.00E+00	1.04E+04	8.08E+08
885.00	1.36E+06	2.61E+06	0.00E+00	2.61E+05	1.57E+06	2.61E+06	5.74E+06	0.00E+00	1.04E+06	5.22E+05	0.00E+00	0.00E+00	0.00E+00	6.26E+05	3.46E+08
881.00	2.09E+06	5.22E+05	0.00E+00	3.13E+05	1.30E+06	5.95E+06	3.65E+06	6.79E+06	1.57E+06	3.13E+05	2.09E+05	0.00E+00	0.00E+00	0.00E+00	2.16E+08
875.75	2.40E+06	4.28E+05	0.00E+00	0.00E+00	1.04E+06	2.82E+06	5.74E+06	1.57E+07	1.04E+06	2.09E+05	1.04E+05	2.09E+05	0.00E+00	1.04E+04	2.63E+08
867.63	2.82E+06	5.74E+06	0.00E+00	0.00E+00	7.31E+05	4.18E+06	1.57E+06	1.77E+06	5.22E+05	0.00E+00	1.30E+06	0.00E+00	0.00E+00	0.00E+00	1.73E+08
859.50	3.13E+06	1.64E+06	0.00E+00	2.09E+05	1.04E+06	3.13E+06	2.09E+06	4.70E+06	7.31E+05	0.00E+00	5.22E+05	0.00E+00	0.00E+00	0.00E+00	2.69E+08
853.00	5.22E+06	2.09E+06	0.00E+00	3.13E+05	3.13E+05	2.09E+06	1.57E+06	4.18E+06	1.77E+06	2.09E+05	2.09E+06	0.00E+00	0.00E+00	0.00E+00	2.15E+08
846.50	4.91E+06	5.74E+06	1.57E+06	2.61E+05	1.36E+06	2.40E+06	3.45E+06	6.79E+06	2.35E+06	0.00E+00	1.57E+06	0.00E+00	0.00E+00	0.00E+00	1.16E+08
842.55	6.79E+06	3.86E+06	0.00E+00	1.04E+06	5.22E+04	2.61E+06	1.77E+06	1.36E+07	1.57E+06	0.00E+00	1.04E+06	0.00E+00	0.00E+00	0.00E+00	1.13E+08
838.60	3.86E+06	2.71E+06	0.00E+00	2.09E+05	4.18E+05	2.40E+06	2.82E+06	2.40E+06	2.35E+06	0.00E+00	2.09E+06	0.00E+00	0.00E+00	0.00E+00	2.09E+08
834.70	6.79E+06	4.44E+06	0.00E+00	2.61E+05	3.13E+05	5.22E+05	2.82E+06	1.04E+07	1.36E+06	0.00E+00	2.09E+06	0.00E+00	0.00E+00	0.00E+00	2.23E+08
830.80	5.95E+06	2.92E+06	0.00E+00	0.00E+00	5.22E+05	1.30E+06	8.66E+06	2.87E+06	7.83E+05	0.00E+00	0.00E+00	0.00E+00	0.00E+00	1.04E+04	3.39E+08
823.00	4.18E+06	2.61E+06	0.00E+00	0.00E+00	6.26E+05	1.04E+06	5.53E+06	3.13E+05	5.22E+05	0.00E+00	0.00E+00	0.00E+00	0.00E+00	5.22E+05	3.38E+08
819.10	3.86E+06	2.92E+05	0.00E+00	1.46E+05	0.00E+00	1.77E+06	2.82E+06	7.31E+05	1.36E+06	0.00E+00	0.00E+00	0.00E+00	0.00E+00	1.04E+05	5.67E+08
815.20	7.83E+05	4.96E+06	0.00E+00	3.13E+05	7.83E+05	1.57E+06	2.82E+06	2.09E+06	7.31E+05	0.00E+00	0.00E+00	0.00E+00	0.00E+00	0.00E+00	3.12E+08
811.30	1.88E+06	2.61E+06	0.00E+00	0.00E+00	0.00E+00	2.61E+06	1.36E+06	2.40E+06	0.00E+00	1.04E+05	0.00E+00	0.00E+00	0.00E+00	0.00E+00	2.20E+08
807.40	4.91E+06	2.51E+06	0.00E+00	0.00E+00	8.35E+05	2.82E+06	1.04E+06	5.22E+05	1.36E+06	0.00E+00	0.00E+00	0.00E+00	0.00E+00	0.00E+00	1.04E+08
803.50	6.99E+06	2.71E+06	0.00E+00	6.26E+05	1.36E+06	4.70E+06	3.13E+05	0.00E+00	1.83E+06	3.13E+05	0.00E+00	0.00E+00	0.00E+00	2.61E+05	1.51E+08
799.60	1.10E+07	2.51E+06	0.00E+00	0.00E+00	5.22E+05	4.70E+06	3.13E+05	1.77E+06	5.22E+05	0.00E+00	0.00E+00	0.00E+00	0.00E+00	0.00E+00	1.51E+08
795.70	7.31E+05	7.31E+05	0.00E+00	0.00E+00	1.67E+05	4.18E+06	3.13E+05	3.13E+05	1.46E+06	0.00E+00	0.00E+00	0.00E+00	0.00E+00	0.00E+00	1.36E+08
789.90	2.92E+05	5.95E+05	1.46E+05	1.30E+05	0.00E+00	2.71E+06	2.61E+05	2.61E+06	3.13E+05	0.00E+00	0.00E+00	0.00E+00	0.00E+00	0.00E+00	9.11E+07
784.00	5.22E+05	1.36E+06	0.00E+00	1.67E+05	3.13E+05	3.86E+06	0.00E+00	1.67E+06	4.38E+05	0.00E+00	0.00E+00	0.00E+00	0.00E+00	0.00E+00	6.54E+07
779.20	0.00E+00	7.41E+05	0.00E+00	0.00E+00	3.13E+05	1.04E+06	0.00E+00	1.04E+06	1.36E+06	0.00E+00	0.00E+00	0.00E+00	0.00E+00	0.00E+00	4.00E+07
774.60	6.26E+05	8.35E+05	0.00E+00	0.00E+00	7.31E+05	3.45E+06	0.00E+00	2.09E+06	5.22E+05	0.00E+00	0.00E+00	0.00E+00	0.00E+00	0.00E+00	6.98E+07

(continued on next page)

Appendix B (*continued*)

Depth (cm)	*Sphenolithus* (/g)	*D. variabilis* (/g)	*D. pentaradiatus* (/g)	*D. brouweri* (/g)	*Pontosphaera* (/g)	*Syracosphaera* (/g)	*G. rotula* (/g)	*G. jafari* (/g)	*R. clavigera* (/g)	*Calciosolenia* (/g)	*R. rotaria* (/g)	*L. perdurum* (/g)	*H. macroporus* (/g)	*Amaurolithus* (/g)	TOTAL (liths/g)
768.40	1.04E+06	1.88E+06	1.67E+05	7.31E+05	1.15E+05	3.13E+06	0.00E+00	8.35E+06	1.83E+06	0.00E+00	0.00E+00	0.00E+00	0.00E+00	0.00E+00	6.94E+07
765.20	5.22E+05	7.41E+05	0.00E+00	2.30E+05	3.13E+05	3.76E+06	7.31E+04	4.18E+06	3.13E+06	0.00E+00	0.00E+00	0.00E+00	0.00E+00	0.00E+00	4.77E+07
760.60	1.25E+06	1.46E+06	0.00E+00	0.00E+00	0.00E+00	2.61E+06	7.31E+05	1.77E+06	5.22E+05	0.00E+00	0.00E+00	0.00E+00	0.00E+00	0.00E+00	5.27E+07
756.00	3.13E+05	3.55E+06	0.00E+00	2.92E+05	4.18E+05	5.22E+06	0.00E+00	3.34E+07	1.04E+06	2.61E+05	3.13E+05	0.00E+00	0.00E+00	0.00E+00	1.01E+08
749.50	2.09E+05	4.59E+05	0.00E+00	0.00E+00	6.26E+05	2.35E+06	0.00E+00	3.13E+06	3.13E+05	5.22E+05	0.00E+00	0.00E+00	0.00E+00	0.00E+00	5.44E+07
746.25	0.00E+00	2.09E+05	0.00E+00	0.00E+00	7.83E+05	3.13E+06	0.00E+00	2.09E+06	1.57E+06	3.13E+05	1.04E+04	1.36E+05	0.00E+00	0.00E+00	7.43E+07
743.00	5.22E+05	1.25E+05	0.00E+00	4.18E+04	1.04E+06	3.86E+06	0.00E+00	1.36E+06	4.18E+05	0.00E+00	0.00E+00	0.00E+00	1.04E+05	0.00E+00	4.66E+07
739.75	6.26E+05	4.38E+05	0.00E+00	0.00E+00	1.57E+06	3.13E+06	3.13E+05	5.22E+05	1.36E+06	0.00E+00	0.00E+00	1.04E+05	0.00E+00	0.00E+00	7.14E+07
736.50	3.13E+05	7.31E+05	0.00E+00	3.13E+05	4.96E+06	3.45E+06	1.36E+06	1.04E+06	5.22E+05	0.00E+00	0.00E+00	0.00E+00	0.00E+00	0.00E+00	7.43E+07
733.25	1.04E+06	2.61E+05	0.00E+00	0.00E+00	1.25E+07	5.74E+06	1.04E+06	2.61E+05	2.09E+05	4.18E+05	0.00E+00	0.00E+00	1.04E+05	0.00E+00	5.34E+07
729.13	2.09E+05	5.22E+04	0.00E+00	0.00E+00	1.88E+07	3.45E+06	5.22E+05	0.00E+00	5.22E+05	0.00E+00	0.00E+00	6.26E+04	5.22E+04	0.00E+00	1.02E+08
725.00	5.22E+05	1.04E+05	0.00E+00	0.00E+00	2.30E+07	2.61E+06	7.31E+05	0.00E+00	1.04E+06	3.13E+05	0.00E+00	0.00E+00	0.00E+00	0.00E+00	9.98E+07
720.00	7.31E+05	3.13E+05	0.00E+00	0.00E+00	4.70E+06	1.77E+06	1.77E+06	0.00E+00	1.04E+06	0.00E+00	0.00E+00	0.00E+00	0.00E+00	0.00E+00	1.18E+08
715.00	3.13E+05	1.04E+05	0.00E+00	2.61E+05	1.57E+06	2.40E+06	5.22E+05	0.00E+00	1.04E+06	0.00E+00	0.00E+00	5.22E+04	0.00E+00	0.00E+00	9.54E+07
710.00	5.22E+05	1.67E+05	0.00E+00	1.25E+05	1.04E+06	1.25E+06	1.77E+05	1.77E+05	1.67E+06	3.13E+05	0.00E+00	0.00E+00	0.00E+00	0.00E+00	5.84E+07
705.00	0.00E+00	0.00E+00	0.00E+00	0.00E+00	7.83E+05	1.77E+06	3.13E+05	0.00E+00	1.04E+06	0.00E+00	3.13E+05	0.00E+00	0.00E+00	0.00E+00	8.74E+07
700.91	5.22E+05	1.57E+05	5.22E+04	0.00E+00	2.40E+06	7.83E+05	0.00E+00	3.13E+05	0.00E+00	7.31E+05	0.00E+00	0.00E+00	0.00E+00	0.00E+00	1.33E+08
696.78	1.04E+06	3.13E+05	0.00E+00	3.13E+05	1.46E+06	4.18E+06	7.31E+05	3.13E+06	7.31E+05	0.00E+00	2.61E+05	0.00E+00	0.00E+00	0.00E+00	2.94E+08
688.52	1.57E+06	8.87E+05	0.00E+00	0.00E+00	6.26E+05	2.09E+06	3.13E+06	0.00E+00	3.13E+05	3.13E+05	0.00E+00	0.00E+00	3.13E+05	0.00E+00	4.77E+08
684.39	1.04E+06	1.57E+05	1.04E+05	5.22E+04	7.83E+05	4.70E+06	2.09E+06	2.09E+06	1.36E+06	7.31E+05	0.00E+00	0.00E+00	0.00E+00	0.00E+00	6.78E+08
680.26	3.13E+05	6.89E+05	0.00E+00	0.00E+00	2.09E+06	2.61E+06	1.04E+06	2.40E+06	5.22E+05	3.13E+05	7.31E+05	0.00E+00	0.00E+00	0.00E+00	5.05E+08
676.13	1.04E+06	7.31E+04	0.00E+00	0.00E+00	5.95E+05	1.04E+06	1.36E+06	7.31E+05	7.31E+05	3.13E+05	3.13E+05	0.00E+00	0.00E+00	0.00E+00	2.95E+08
672.00	7.31E+05	0.00E+00	0.00E+00	0.00E+00	1.67E+05	6.89E+05	1.36E+06	1.36E+06	1.04E+06	0.00E+00	0.00E+00	0.00E+00	2.09E+05	0.00E+00	4.24E+08
668.50	3.39E+06	2.09E+06	0.00E+00	2.61E+05	1.30E+06	5.22E+06	2.82E+06	0.00E+00	2.87E+06	2.40E+06	1.57E+06	0.00E+00	0.00E+00	5.22E+04	4.65E+08
664.75	8.04E+06	9.40E+06	3.13E+06	7.83E+05	2.09E+05	2.82E+06	4.91E+06	1.36E+06	3.45E+06	5.22E+05	2.87E+06	0.00E+00	1.04E+05	6.26E+04	1.46E+08
661.00	3.65E+06	4.49E+06	1.77E+06	1.77E+06	2.92E+05	2.09E+06	1.25E+06	3.45E+06	1.77E+06	3.13E+05	1.67E+06	0.00E+00	0.00E+00	0.00E+00	1.35E+08
651.26	1.77E+06	5.22E+06	1.30E+06	1.57E+06	7.31E+05	1.77E+06	3.86E+06	2.09E+06	1.83E+06	0.00E+00	0.00E+00	0.00E+00	0.00E+00	0.00E+00	9.07E+07
646.40	2.09E+06	4.70E+06	8.35E+05	4.18E+05	0.00E+00	5.22E+05	2.61E+06	1.30E+06	1.77E+06	0.00E+00	0.00E+00	0.00E+00	0.00E+00	1.04E+05	1.36E+08
642.78	1.36E+06	4.18E+06	3.65E+06	1.04E+06	1.04E+05	1.30E+06	2.40E+06	2.82E+06	2.09E+06	5.22E+05	0.00E+00	0.00E+00	0.00E+00	0.00E+00	1.32E+08
639.16	1.57E+06	2.87E+06	8.35E+06	1.30E+06	1.36E+06	2.61E+06	1.57E+06	1.04E+06	6.26E+05	0.00E+00	0.00E+00	0.00E+00	0.00E+00	0.00E+00	1.10E+08
635.54	1.57E+06	8.09E+06	2.35E+06	2.35E+06	0.00E+00	5.22E+05	3.45E+06	6.26E+05	0.00E+00	1.04E+06	0.00E+00	0.00E+00	0.00E+00	1.04E+05	1.71E+08
631.92	6.26E+05	5.74E+06	1.04E+06	0.00E+00	1.46E+05	3.13E+06	2.40E+06	0.00E+00	1.36E+06	3.13E+05	0.00E+00	0.00E+00	0.00E+00	1.67E+05	1.76E+08
628.30	2.40E+06	2.09E+06	2.92E+06	8.66E+05	1.36E+06	5.22E+06	2.09E+06	1.36E+06	1.04E+06	0.00E+00	0.00E+00	2.09E+05	0.00E+00	0.00E+00	9.34E+07
624.68	7.31E+05	2.09E+06	6.26E+05	3.13E+05	1.04E+06	1.77E+06	2.09E+06	1.57E+06	5.22E+05	0.00E+00	1.04E+06	0.00E+00	3.13E+05	0.00E+00	1.64E+08
617.44	8.35E+06	1.57E+06	1.04E+06	0.00E+00	2.61E+05	1.04E+06	4.18E+06	1.04E+06	5.22E+05	5.22E+05	0.00E+00	0.00E+00	0.00E+00	0.00E+00	1.31E+08
613.82	6.79E+06	1.04E+06	7.31E+05	0.00E+00	7.31E+05	1.04E+06	3.13E+06	2.09E+06	4.80E+06	3.13E+05	0.00E+00	0.00E+00	0.00E+00	0.00E+00	2.49E+08
610.20	6.26E+06	5.22E+05	0.00E+00	0.00E+00	0.00E+00	6.26E+06	7.31E+06	5.22E+05	3.13E+05	3.13E+05	3.13E+05	0.00E+00	0.00E+00	0.00E+00	2.46E+08
606.58	8.87E+06	8.35E+05	1.04E+06	0.00E+00	0.00E+00	1.04E+06	2.82E+06	0.00E+00	1.04E+05	0.00E+00	0.00E+00	0.00E+00	0.00E+00	1.04E+05	1.37E+08
602.96	5.22E+06	3.42E+06	1.67E+05	0.00E+00	5.22E+05	2.61E+06	2.61E+06	0.00E+00	5.22E+05	0.00E+00	5.22E+05	0.00E+00	0.00E+00	0.00E+00	1.77E+08
599.34	9.40E+06	2.61E+05	2.09E+04	0.00E+00	7.31E+05	2.40E+06	1.36E+06	2.09E+06	1.36E+06	1.04E+06	0.00E+00	0.00E+00	0.00E+00	1.04E+05	1.52E+08
595.72	1.28E+07	5.74E+06	0.00E+00	7.83E+05	4.91E+06	3.76E+06	3.13E+06	1.88E+07	2.40E+06	3.86E+06	0.00E+00	0.00E+00	0.00E+00	0.00E+00	2.12E+08
592.10	8.35E+06	3.76E+06	0.00E+00	6.26E+05	3.86E+06	4.18E+06	1.04E+06	1.04E+07	1.57E+06	1.57E+06	0.00E+00	0.00E+00	0.00E+00	0.00E+00	1.69E+08
584.86	0.00E+00	2.82E+06	5.22E+04	1.25E+06	4.70E+06	3.13E+06	5.22E+06	7.31E+05	0.00E+00	0.00E+00	0.00E+00	0.00E+00	0.00E+00	0.00E+00	2.59E+08
581.24	1.30E+06	6.52E+06	1.04E+05	5.22E+04	2.40E+06	3.13E+06	6.58E+06	0.00E+00	5.22E+05	1.04E+06	1.04E+06	0.00E+00	0.00E+00	0.00E+00	2.55E+08
577.62	1.36E+06	4.96E+06	0.00E+00	5.22E+05	4.18E+06	7.83E+06	2.56E+07	0.00E+00	4.80E+06	1.67E+06	0.00E+00	0.00E+00	0.00E+00	0.00E+00	3.96E+08
574.00	1.46E+05	3.13E+06	0.00E+00	0.00E+00	2.40E+06	2.40E+06	4.49E+06	7.31E+05	1.36E+06	1.36E+06	0.00E+00	1.04E+05	3.13E+05	2.61E+05	2.84E+08
570.10	5.22E+05	1.25E+06	0.00E+00	0.00E+00	2.40E+06	4.70E+06	7.93E+06	0.00E+00	5.22E+05	2.61E+06	0.00E+00	3.13E+05	2.09E+05	0.00E+00	3.70E+08

566.20	2.51E+05	2.09E+06	0.00E+00	0.00E+00	1.67E+06	1.25E+07	8.35E+06	0.00E+00	1.83E+06	2.61E+05	0.00E+00	0.00E+00	5.22E+05	0.00E+00	3.05E+08
562.38	5.22E+05	1.48E+06	0.00E+00	0.00E+00	2.61E+06	3.45E+06	7.62E+06	0.00E+00	1.36E+06	2.09E+06	0.00E+00	1.04E+05	0.00E+00	0.00E+00	2.57E+08
558.56	1.57E+06	4.59E+05	0.00E+00	0.00E+00	8.04E+06	3.76E+06	1.57E+07	1.57E+07	1.36E+06	1.36E+06	0.00E+00	0.00E+00	0.00E+00	0.00E+00	3.72E+08
550.92	7.31E+05	5.95E+05	0.00E+00	0.00E+00	7.31E+06	2.61E+06	1.30E+07	1.04E+06	1.36E+06	1.04E+06	0.00E+00	0.00E+00	0.00E+00	0.00E+00	2.73E+08
547.10	0.00E+00	8.35E+05	0.00E+00	0.00E+00	5.85E+06	3.65E+06	1.20E+07	0.00E+00	1.67E+06	1.83E+06	0.00E+00	1.04E+05	0.00E+00	0.00E+00	1.80E+08
543.28	3.86E+05	8.35E+05	0.00E+00	0.00E+00	4.18E+06	4.18E+06	7.31E+06	0.00E+00	7.31E+05	2.09E+06	0.00E+00	0.00E+00	0.00E+00	0.00E+00	1.36E+08
539.46	2.61E+05	8.35E+05	0.00E+00	1.04E+05	1.36E+07	3.13E+06	2.57E+07	1.04E+06	1.04E+06	1.36E+06	0.00E+00	0.00E+00	0.00E+00	0.00E+00	5.20E+08
535.64	5.22E+05	1.67E+06	0.00E+00	0.00E+00	1.70E+07	3.13E+06	3.45E+07	0.00E+00	1.67E+06	3.13E+05	0.00E+00	1.04E+05	0.00E+00	0.00E+00	1.05E+08
531.82	4.18E+05	9.08E+05	0.00E+00	0.00E+00	8.66E+06	6.26E+06	1.15E+07	0.00E+00	7.83E+05	1.04E+06	0.00E+00	1.04E+05	0.00E+00	0.00E+00	6.99E+07
528.21	0.00E+00	1.21E+06	0.00E+00	0.00E+00	1.77E+07	1.04E+07	2.45E+07	1.36E+06	1.30E+06	0.00E+00	0.00E+00	0.00E+00	0.00E+00	0.00E+00	1.50E+08
524.61	5.22E+05	3.13E+06	0.00E+00	0.00E+00	1.36E+07	9.40E+06	5.95E+06	8.66E+06	5.22E+05	0.00E+00	0.00E+00	8.35E+05	6.26E+05	0.00E+00	1.23E+08
521.00	3.76E+05	0.00E+00	0.00E+00	0.00E+00	5.95E+06	5.74E+06	1.77E+06	4.18E+06	6.26E+05	5.22E+05	0.00E+00	0.00E+00	5.22E+05	0.00E+00	1.17E+08
515.00	0.00E+00	3.13E+05	1.04E+05	0.00E+00	1.36E+06	4.70E+06	1.77E+06	1.39E+07	0.00E+00	1.04E+06	0.00E+00	0.00E+00	0.00E+00	0.00E+00	8.32E+07
509.00	7.83E+05	3.86E+05	0.00E+00	1.30E+05	7.83E+05	1.57E+06	5.22E+05	3.39E+06	0.00E+00	0.00E+00	0.00E+00	0.00E+00	0.00E+00	5.22E+05	7.98E+07
503.00	6.26E+05	1.67E+06	0.00E+00	0.00E+00	1.67E+06	3.13E+06	7.31E+05	1.15E+07	1.04E+06	0.00E+00	5.22E+05	0.00E+00	1.04E+05	0.00E+00	2.98E+08
497.00	5.95E+06	1.04E+06	1.04E+05	0.00E+00	8.35E+05	1.04E+06	1.36E+06	8.35E+06	1.04E+06	1.04E+06	3.13E+05	0.00E+00	1.04E+05	5.22E+05	1.97E+08
491.00	3.13E+06	1.04E+06	1.77E+06	0.00E+00	6.26E+05	2.40E+06	1.04E+06	1.77E+06	3.13E+05	3.13E+05	0.00E+00	0.00E+00	0.00E+00	0.00E+00	1.69E+08
485.00	5.22E+06	1.04E+06	3.13E+05	0.00E+00	1.04E+06	1.57E+06	1.77E+06	3.13E+06	5.22E+05	0.00E+00	1.04E+06	0.00E+00	0.00E+00	0.00E+00	2.36E+08
480.50	5.74E+06	1.25E+06	4.18E+05	0.00E+00	1.57E+06	3.13E+06	1.04E+06	1.30E+06	5.22E+05	2.09E+05	3.13E+05	0.00E+00	0.00E+00	0.00E+00	4.21E+08
476.00	4.91E+06	5.22E+04	3.76E+05	0.00E+00	0.00E+00	5.22E+05	1.04E+06	6.79E+06	1.04E+06	0.00E+00	1.04E+06	0.00E+00	0.00E+00	0.00E+00	6.59E+08
467.00	3.13E+06	4.38E+06	2.71E+06	2.09E+05	2.61E+06	3.76E+06	1.77E+06	3.13E+05	1.36E+06	5.22E+05	2.61E+06	0.00E+00	0.00E+00	0.00E+00	2.95E+08
462.50	1.36E+06	8.09E+06	3.91E+06	0.00E+00	2.61E+06	2.09E+06	2.82E+06	1.77E+06	3.86E+06	2.09E+06	3.13E+06	0.00E+00	0.00E+00	0.00E+00	1.78E+08
458.00	2.61E+06	3.97E+06	5.01E+06	4.18E+05	2.40E+06	9.08E+06	3.45E+06	1.04E+06	5.22E+06	4.91E+06	1.04E+06	0.00E+00	0.00E+00	0.00E+00	9.71E+07
453.00	2.09E+06	6.00E+06	3.91E+06	5.22E+05	2.09E+06	3.65E+06	3.86E+06	0.00E+00	3.13E+06	1.57E+06	0.00E+00	1.04E+05	0.00E+00	0.00E+00	1.61E+08
448.00	4.18E+05	5.22E+05	5.22E+05	0.00E+00	8.35E+05	1.57E+06	3.86E+06	0.00E+00	2.09E+06	1.57E+06	5.22E+05	0.00E+00	0.00E+00	0.00E+00	6.74E+07
443.00	4.91E+06	4.44E+06	0.00E+00	1.83E+06	2.82E+06	5.53E+06	2.82E+06	7.31E+05	5.53E+06	5.22E+06	0.00E+00	0.00E+00	0.00E+00	6.26E+05	8.87E+07
438.00	2.61E+06	2.92E+06	4.18E+05	8.35E+05	2.82E+06	2.09E+06	2.40E+06	3.13E+05	3.86E+06	2.82E+06	0.00E+00	0.00E+00	0.00E+00	5.22E+05	1.04E+08
428.00	1.57E+06	6.58E+06	5.22E+04	1.04E+06	6.99E+06	4.18E+06	5.22E+06	0.00E+00	3.45E+06	9.71E+06	0.00E+00	0.00E+00	0.00E+00	3.13E+05	1.90E+08
421.90	3.86E+06	3.13E+06	0.00E+00	1.67E+05	2.82E+06	5.22E+06	1.77E+06	1.04E+06	1.57E+06	5.74E+06	0.00E+00	0.00E+00	0.00E+00	0.00E+00	8.01E+07
415.80	3.13E+05	1.88E+06	0.00E+00	0.00E+00	6.26E+05	2.09E+06	4.49E+06	0.00E+00	1.36E+06	3.39E+06	0.00E+00	0.00E+00	0.00E+00	0.00E+00	1.22E+08
409.70	2.40E+06	1.88E+06	0.00E+00	5.22E+05	1.57E+06	3.45E+06	3.45E+06	0.00E+00	3.13E+05	3.13E+06	0.00E+00	0.00E+00	0.00E+00	0.00E+00	1.56E+08
405.12	1.36E+06	2.61E+06	0.00E+00	0.00E+00	0.00E+00	1.77E+06	4.18E+06	0.00E+00	2.82E+06	3.86E+06	3.13E+06	0.00E+00	0.00E+00	0.00E+00	2.59E+08
400.54	3.13E+06	5.48E+06	5.22E+05	0.00E+00	4.49E+05	5.22E+05	3.13E+06	6.26E+05	2.09E+06	1.36E+06	0.00E+00	0.00E+00	0.00E+00	0.00E+00	1.41E+08
395.96	5.22E+05	2.71E+06	6.26E+05	2.09E+05	2.92E+05	2.40E+06	3.13E+06	0.00E+00	3.13E+06	6.99E+06	3.13E+05	0.00E+00	0.00E+00	0.00E+00	1.67E+08
391.38	1.57E+06	3.76E+06	0.00E+00	4.18E+05	4.38E+05	1.67E+06	2.61E+06	3.86E+06	1.77E+06	5.22E+06	0.00E+00	0.00E+00	0.00E+00	0.00E+00	1.47E+08
386.80	1.51E+07	4.44E+06	1.30E+06	5.22E+05	2.61E+05	4.70E+06	3.13E+06	2.82E+06	2.09E+06	1.57E+06	0.00E+00	0.00E+00	0.00E+00	0.00E+00	1.29E+08
377.64	1.67E+06	1.57E+06	1.21E+06	2.09E+05	1.04E+06	6.58E+06	7.83E+05	2.40E+07	1.25E+07	2.09E+06	0.00E+00	0.00E+00	0.00E+00	0.00E+00	1.72E+08
373.06	4.18E+06	1.67E+06	1.67E+06	0.00E+00	3.13E+05	2.09E+06	2.40E+06	8.35E+06	2.09E+06	0.00E+00	5.22E+05	0.00E+00	0.00E+00	0.00E+00	1.85E+08
368.48	9.40E+06	2.09E+06	1.04E+06	0.00E+00	0.00E+00	1.67E+06	3.13E+05	3.86E+06	1.36E+06	0.00E+00	5.22E+05	0.00E+00	0.00E+00	0.00E+00	1.50E+08
363.90	2.82E+06	4.38E+05	2.92E+05	0.00E+00	0.00E+00	2.09E+06	1.83E+06	1.30E+06	7.31E+05	7.31E+05	0.00E+00	0.00E+00	0.00E+00	0.00E+00	2.23E+08
359.32	4.49E+06	1.21E+06	2.92E+05	0.00E+00	3.13E+05	1.73E+06	2.40E+06	3.13E+06	2.09E+06	1.04E+06	0.00E+00	0.00E+00	0.00E+00	0.00E+00	3.52E+08
354.74	2.40E+06	2.30E+06	7.31E+05	0.00E+00	3.13E+05	2.71E+06	1.67E+06	3.45E+06	3.13E+06	1.04E+06	0.00E+00	0.00E+00	0.00E+00	0.00E+00	2.08E+08
349.31	1.67E+07	2.30E+06	6.26E+05	0.00E+00	5.22E+05	3.13E+06	3.13E+05	2.82E+06	1.04E+06	3.13E+05	0.00E+00	0.00E+00	0.00E+00	4.18E+05	9.40E+07
343.88	1.15E+07	2.30E+06	5.22E+05	0.00E+00	1.04E+06	3.13E+06	0.00E+00	4.80E+07	1.67E+06	6.26E+05	0.00E+00	0.00E+00	0.00E+00	1.04E+04	2.50E+08
333.03	2.09E+06	2.09E+05	0.00E+00	0.00E+00	3.13E+05	4.70E+06	0.00E+00	3.65E+07	1.57E+06	8.35E+05	5.22E+05	0.00E+00	0.00E+00	0.00E+00	1.44E+08
327.60	4.44E+06	7.31E+05	0.00E+00	1.57E+05	7.83E+05	1.04E+06	0.00E+00	2.40E+06	7.31E+05	4.18E+05	0.00E+00	0.00E+00	0.00E+00	5.22E+04	2.34E+08
321.00	4.49E+06	2.09E+05	0.00E+00	6.26E+04	1.04E+06	2.09E+06	0.00E+00	3.13E+06	5.22E+05	1.04E+06	1.04E+04	5.22E+04	0.00E+00	0.00E+00	3.14E+08
317.55	1.30E+06	7.31E+05	0.00E+00	7.31E+05	1.57E+06	1.67E+06	0.00E+00	1.46E+07	2.09E+05	0.00E+00	0.00E+00	2.09E+05	0.00E+00	0.00E+00	8.84E+07
314.10	7.31E+06	2.09E+06	0.00E+00	1.04E+06	3.13E+05	3.45E+06	5.22E+04	4.49E+06	1.77E+06	0.00E+00	0.00E+00	0.00E+00	0.00E+00	0.00E+00	8.61E+07
310.65	6.26E+05	1.57E+06	0.00E+00	1.67E+05	1.04E+06	4.49E+06	0.00E+00	9.92E+06	0.00E+00	0.00E+00	0.00E+00	0.00E+00	0.00E+00	0.00E+00	6.48E+07

(continued on next page)

Appendix B (*continued*)

Depth (cm)	*Sphenolithus* (/g)	*D. variabilis* (/g)	*D. pentaradiatus* (/g)	*D. brouweri* (/g)	*Pontosphaera* (/g)	*Syracosphaera* (/g)	*G. rotula* (/g)	*G. jafari* (/g)	*R. clavigera* (/g)	*Calciosolenia* (/g)	*R. rotaria* (/g)	*L. perdurum* (/g)	*H. macroporus* (/g)	*Amaurolithus* (/g)	TOTAL (liths/g)
307.20	6.26E+04	2.09E+06	0.00E+00	0.00E+00	5.22E+05	2.82E+06	2.61E+05	1.77E+07	1.25E+06	2.09E+05	0.00E+00	0.00E+00	0.00E+00	0.00E+00	7.90E+07
298.60	8.66E+05	5.22E+05	0.00E+00	0.00E+00	8.35E+05	1.57E+06	0.00E+00	6.58E+06	8.35E+05	7.31E+05	0.00E+00	0.00E+00	0.00E+00	0.00E+00	4.27E+07
290.00	5.22E+05	1.15E+06	0.00E+00	3.13E+05	1.04E+06	3.13E+06	1.36E+06	2.51E+07	2.40E+06	5.22E+05	5.22E+05	0.00E+00	0.00E+00	0.00E+00	8.68E+07
285.25	4.18E+05	3.13E+05	7.31E+05	2.40E+06	5.22E+05	5.43E+07	0.00E+00	0.00E+00	0.00E+00	0.00E+00	0.00E+00	0.00E+00	0.00E+00	0.00E+00	9.54E+07
280.50	3.13E+05	2.71E+05	0.00E+00	6.26E+04	1.25E+05	2.09E+06	3.13E+05	2.87E+07	1.04E+06	2.61E+05	0.00E+00	0.00E+00	0.00E+00	0.00E+00	7.08E+07
274.66	0.00E+00	2.09E+05	0.00E+00	5.22E+04	1.04E+06	2.09E+06	2.09E+06	2.66E+07	1.04E+06	0.00E+00	0.00E+00	0.00E+00	0.00E+00	0.00E+00	7.26E+07
268.83	1.04E+06	6.26E+04	5.22E+04	5.22E+04	7.31E+05	2.61E+06	7.83E+05	2.19E+07	6.26E+05	1.04E+06	0.00E+00	0.00E+00	0.00E+00	0.00E+00	1.01E+08
263.00	5.22E+05	1.57E+05	5.22E+04	0.00E+00	2.09E+06	7.31E+05	4.18E+06	3.86E+06	2.40E+06	0.00E+00	0.00E+00	0.00E+00	0.00E+00	0.00E+00	5.94E+07
253.00	0.00E+00	1.67E+05	5.22E+04	1.04E+05	2.09E+06	1.77E+06	7.31E+05	2.09E+06	0.00E+00	6.26E+05	0.00E+00	0.00E+00	0.00E+00	0.00E+00	8.18E+07
241.00	5.22E+05	2.30E+05	3.13E+05	0.00E+00	5.22E+05	1.04E+06	0.00E+00	1.04E+06	0.00E+00	0.00E+00	0.00E+00	0.00E+00	0.00E+00	0.00E+00	5.48E+07
235.20	0.00E+00	1.36E+05	0.00E+00	6.26E+04	0.00E+00	1.04E+06	7.83E+05	5.22E+05	2.09E+05	0.00E+00	0.00E+00	0.00E+00	1.04E+05	0.00E+00	5.80E+07
223.60	3.13E+05	5.95E+05	1.88E+05	5.22E+04	3.13E+05	5.22E+04	1.25E+06	5.22E+05	5.22E+05	0.00E+00	5.22E+05	0.00E+00	0.00E+00	0.00E+00	4.72E+08
219.73	3.13E+05	1.04E+05	0.00E+00	5.22E+05	0.00E+00	0.00E+00	5.22E+05	0.00E+00	0.00E+00	0.00E+00	0.00E+00	0.00E+00	0.00E+00	0.00E+00	3.90E+08
212.00	1.57E+06	0.00E+00	5.22E+05	0.00E+00	1.36E+06	4.18E+05	3.13E+05	0.00E+00	7.31E+05	3.13E+05	5.22E+05	0.00E+00	0.00E+00	0.00E+00	2.28E+08
204.00	9.40E+06	3.13E+05	2.61E+05	2.61E+05	2.92E+05	1.04E+06	3.13E+06	2.61E+05	5.22E+05	0.00E+00	3.13E+05	0.00E+00	0.00E+00	0.00E+00	7.42E+08
196.00	3.86E+06	1.67E+05	1.57E+06	5.22E+05	1.04E+06	1.77E+06	2.82E+06	6.26E+05	4.18E+05	1.36E+06	7.31E+05	2.09E+05	0.00E+00	0.00E+00	8.21E+08
180.00	2.09E+06	4.70E+06	1.36E+06	1.25E+06	5.22E+05	2.09E+06	4.18E+06	0.00E+00	2.40E+06	5.22E+05	1.36E+06	0.00E+00	0.00E+00	1.04E+05	4.62E+08
172.00	2.35E+06	1.83E+06	1.83E+06	2.09E+06	1.04E+06	2.40E+06	5.74E+06	1.04E+06	3.45E+06	1.36E+06	3.65E+06	0.00E+00	0.00E+00	0.00E+00	3.73E+08
156.00	4.70E+06	2.09E+06	8.87E+05	1.25E+06	3.13E+05	2.82E+06	6.99E+06	5.22E+05	1.77E+06	1.77E+06	2.09E+06	0.00E+00	0.00E+00	0.00E+00	4.43E+08
150.33	1.57E+06	2.87E+06	1.83E+06	1.57E+06	2.09E+06	3.45E+06	7.62E+06	1.04E+06	3.13E+06	3.13E+05	2.82E+06	0.00E+00	0.00E+00	0.00E+00	3.12E+08
139.00	6.26E+06	4.70E+06	1.77E+06	0.00E+00	0.00E+00	2.09E+06	3.91E+06	1.77E+06	2.09E+06	1.77E+06	1.83E+06	0.00E+00	0.00E+00	1.04E+05	2.12E+08
128.50	3.45E+06	2.09E+06	3.13E+06	0.00E+00	1.36E+06	2.09E+06	4.70E+06	5.22E+05	7.83E+05	0.00E+00	4.70E+06	1.04E+05	0.00E+00	0.00E+00	2.75E+08
123.25	0.00E+00	4.18E+05	8.35E+05	0.00E+00	0.00E+00	5.22E+06	1.36E+06	3.13E+05	1.04E+06	2.61E+05	0.00E+00	0.00E+00	0.00E+00	0.00E+00	2.44E+08
112.75	3.13E+06	1.04E+06	8.35E+05	2.09E+05	0.00E+00	3.13E+06	2.82E+06	1.36E+06	1.57E+06	0.00E+00	0.00E+00	1.04E+05	0.00E+00	1.04E+05	4.32E+08
107.50	5.74E+06	1.30E+06	2.09E+05	0.00E+00	1.04E+06	1.57E+06	1.04E+06	0.00E+00	1.57E+06	0.00E+00	0.00E+00	0.00E+00	0.00E+00	0.00E+00	1.31E+08
103.75	5.53E+06	3.65E+05	8.35E+06	0.00E+00	1.04E+06	1.36E+06	2.71E+06	5.22E+05	2.82E+06	5.22E+05	0.00E+00	0.00E+00	0.00E+00	0.00E+00	3.53E+08
100.00	7.31E+06	5.22E+05	3.55E+06	7.31E+05	5.22E+05	6.89E+06	7.31E+05	5.53E+06	1.04E+06	1.04E+06	0.00E+00	0.00E+00	0.00E+00	0.00E+00	2.04E+08
92.50	3.65E+06	1.36E+06	3.86E+06	0.00E+00	1.30E+06	2.78E+06	1.30E+06	3.13E+05	7.83E+05	1.04E+06	0.00E+00	0.00E+00	0.00E+00	0.00E+00	2.84E+08
88.75	7.83E+06	3.76E+06	0.00E+00	5.22E+05	5.22E+05	2.61E+06	1.36E+06	0.00E+00	1.83E+06	0.00E+00	0.00E+00	0.00E+00	0.00E+00	0.00E+00	1.02E+08
81.25	9.40E+06	2.40E+06	0.00E+00	0.00E+00	0.00E+00	2.40E+06	1.46E+05	1.67E+05	1.04E+06	7.31E+04	0.00E+00	0.00E+00	0.00E+00	0.00E+00	8.84E+07
65.50	2.14E+07	1.88E+06	0.00E+00	6.26E+05	2.61E+05	2.40E+06	5.22E+05	0.00E+00	3.13E+05	4.18E+05	0.00E+00	0.00E+00	0.00E+00	0.00E+00	9.67E+07
60.50	2.09E+06	2.40E+06	0.00E+00	0.00E+00	3.13E+05	6.26E+06	1.83E+06	5.22E+05	2.09E+05	3.13E+05	0.00E+00	0.00E+00	0.00E+00	0.00E+00	1.16E+08

Appendix C. P/Ti ratio, opal, total organic matter and calcium carbonate (%) in the Sorbas basin

Depth (cm)	P/Ti	Opal %	TOC	Depth (cm)	$CaCO_3$ %
972.12	0.3048	1.33	0.67	993.00	37.36
963.58	0.2487	1.13	0.43	988.45	31.09
955.04	0.2489	1.57	0.6	983.67	30.55
946.50	0.2526	1.93	0.22	979.22	31.34
939.50	0.3845	15.73	0.63	974.56	34.57
929.00	0.3517	9.76	0.57	969.78	18.38
922.00	0.3812	6.73	0.36	965.00	27.08
910.68	0.4481	5.39	0.32	961.56	29.23
902.12	0.3630	2.34	0.49	956.67	31.44
893.56	0.3379	1.14	0.66	952.00	32.16
885.00	0.2243	0.1	0.37	946.89	33.64
881.00	0.2701	1.13	0.25	941.89	32.07
875.75	0.3083	1.15	0.32	937.56	36.52
859.50	0.2387	1.05	0.28	934.45	38.70
853.00	0.2526	1.1	0.17	930.89	37.60
846.50	0.2388	1.81	0.22	925.45	43.71
830.80	0.2077	1.4	0.22	920.78	43.88
826.90	0.2761	1.65	0.24	915.89	43.63
819.10	0.3197	1.14	0.28	912.00	47.87
807.40	0.2626	1.29	0.28	907.11	46.50
784.00	0.2266	1.59	0.31	903.00	49.56
774.60	0.2065	1.81	0.27	897.78	51.74
765.20	0.2896	1.44	0.39	891.11	54.67
760.60	0.2721	1.84	0.45	883.78	55.56
756.00	0.2119	1.6	0.41	877.11	48.84
749.50	0.2836	1.27	0.45	873.00	37.84
743.00	0.2996	1.54	0.51	866.33	46.45
739.75	0.2961	1.64	0.54	859.89	46.81
733.25	0.2543	1.62	0.55	854.45	43.13
725.00	0.4060	2.01	0.7	850.78	45.15
710.00	0.3677	8.62	0.67	848.22	41.75
700.91	0.4243	2.36	0.37	843.56	45.65
688.52	0.2867	1.19	0.51	840.22	45.11
684.39	0.3221	1.04	0.43	836.89	44.55
676.13	0.3661	1.02	0.56	833.56	49.44
672.00	0.3887	0.88	0.7	830.11	49.03
661.00	0.2526	1.03	0.22	826.56	43.61
646.40	0.2789	1.04	0.31	823.22	39.48
639.16	0.2309	1.27	0.6	819.56	39.05
631.92	0.2548	1.48	0.23	816.45	43.13
621.06	0.2340	1.31	0.38	809.45	37.25
610.20	0.2501	1.7	0.29	806.11	37.63
599.34	0.2111	1.65	0.27	801.78	38.28
588.48	0.1973	1.43	0.25	795.33	37.46
581.24	0.2427	1.68	0.29	791.11	36.64
574.00	0.2063	0.72	0.29	788.11	36.45
566.20	0.1907	1.65	0.25	784.22	37.34
558.56	0.1731	1.41	0.35	777.45	35.71
550.92	0.2270	1.68	0.25	774.00	35.56
543.28	0.1553	1.69	0.38	769.33	40.24
531.82	0.2683	1.99	0.46	765.22	37.81
521.00	0.3059	6.23	0.47	761.11	39.55
515.00	0.2353	28.44	0.23	759.33	35.36
503.00	0.2941	9.41	1.01	752.55	37.68
491.00	0.3000	2.72	0.46	747.22	37.49
485.00	0.3000	1.03	0.73	742.44	38.74
476.00	0.2778	1.02	0.44	738.89	38.57
467.00	0.1818	2.46	0.57	735.22	36.81
462.50	0.1739	1.53	0.33	730.55	34.31
458.00	0.1905	1.69	0.24	725.44	33.36
448.00	0.2105	1.24	0.38	722.33	30.55
438.00	0.1754	1.67	0.32	717.33	28.83
428.00	0.1739	1.18	0.69	714.11	45.61
409.70	0.2273	1.49	0.29	709.44	44.84
395.96	0.1667	1.53	0.51	700.33	46.90
382.22	0.1600	1.4	0.59	695.00	49.56
368.48	0.1667	1.54	0.29	689.33	54.77
354.74	0.1800	1.67	0.37	683.66	57.93
341.00	0.1923	1.58	0.66	677.66	54.01
327.60	0.1923	1.56	0.35	672.77	39.07
321.00	0.2000	1.59	0.31	668.66	43.04
314.10	0.1685	1.81	0.28	664.44	46.24
307.20	0.1786	1.7	0.5	660.89	41.95
298.60	0.1481	1.69	0.24	652.11	38.87
290.00	0.1923	1.48	0.28	648.22	40.36
280.50	0.1852	1.61	0.42	643.89	42.11
263.00	0.2800	1.3	0.35	639.44	38.10
253.00	0.2727	4.32	0.35	635.55	0.00
241.00	0.2273	4.49	0.39	630.66	42.58
235.20	0.2500	2.77	0.47	627.55	38.86
223.60	0.2388	2.33	0.42	622.66	36.71
214.90	0.2222	1.14	0.5	618.77	37.65
212.00	0.2500	1.6	0.44	615.00	42.14
204.00	0.2353	0.98	0.5	610.33	41.07
196.00	0.2000	0.86	0.59	605.66	44.33
188.00	0.2174	1.62	0.78	602.00	35.47
180.00	0.2083	1.14	1.67	597.89	37.10
156.00	0.2083	1.17	1.89	593.00	34.29
139.00	0.1739	1.51	0.31	589.33	35.90
123.25	0.2000	1.56	1.04	585.22	35.61
107.50	0.1884	1.15	1.2	580.33	35.02
91.75	0.1600	1.5	0.3	576.66	33.11
76.00	0.1481	1.76	0.31	572.11	32.53
81.25	0.2358	1.86	0.27	567.44	33.99
65.50	0.1786	1.85	0.33	564.33	34.83
60.50	0.1538	1.59	0.52	560.66	35.73
47.13	0.1786	1.3	0.35	555.55	37.12
36.88	0.2565	0.91	0.45	550.89	33.85
26.63	0.2400	1.88	0.3	545.77	33.42
16.38	0.2727	1.79	0.33	535.89	34.47
1.00	0.3710	2.03	0.4	533.78	31.67
				530.11	31.00
				526.33	31.71
				523.33	29.65
				520.11	31.21

Appendix C (*continued*)

Depth (cm)	P/Ti	Opal %	TOC	Depth (cm)	$CaCO_3$ %
				515.67	30.07
				511.44	35.28
				507.33	32.18
				500.55	22.97
				494.89	24.96
				488.67	19.45
				482.22	37.02
				477.89	42.67
				473.00	44.93
				468.11	42.00
				462.89	53.79
				458.33	39.90
				453.44	41.44
				450.33	42.24
				446.33	42.44
				441.78	42.37
				436.89	52.50
				431.67	46.70
				426.67	35.04
				416.11	41.79
				411.78	47.35
				407.67	42.27
				402.78	46.25
				398.33	48.51
				394.22	43.24
				389.55	44.85
				384.89	41.25
				380.33	39.60
				376.00	34.82
				371.44	37.02
				367.89	36.69
				363.44	42.07
				358.67	43.35
				354.11	44.06
				350.33	40.66
				346.00	37.54
				341.22	36.99
				336.67	33.86
				331.00	37.28
				325.55	39.26
				320.11	39.76
				316.44	35.64
				312.11	34.18
				307.11	32.87
				303.00	35.62
				298.11	31.57
				294.33	33.14
				288.89	35.80
				282.89	33.86
				279.00	33.20
				273.89	34.17
				268.67	34.06
				256.11	35.45
				251.11	33.79

Appendix C (*continued*)

Depth (cm)	P/Ti	Opal %	TOC	Depth (cm)	$CaCO_3$ %
				245.44	34.23
				238.44	36.01
				231.56	33.32
				226.67	33.52
				220.67	35.46
				215.22	42.12
				209.33	52.10
				202.56	42.71
				197.67	46.23
				193.33	53.49
				188.11	46.51
				184.00	43.00
				177.33	39.96
				169.89	32.47
				165.44	41.85
				160.56	33.04
				154.89	25.05
				149.89	41.12
				144.67	32.74
				139.33	41.34
				133.44	41.47
				128.44	30.33
				122.78	42.93
				117.56	27.56
				112.22	24.89
				106.78	21.59
				101.11	26.73
				95.89	31.73
				90.78	20.05
				85.33	22.12
				80.00	18.33
				70.22	21.90
				68.78	21.70
				62.89	21.31
				58.78	21.48
				53.67	21.35
				43.44	22.69
				38.89	24.39
				34.44	23.90
				29.78	23.25
				25.11	23.46
				19.78	23.14
				14.56	26.09
				11.00	28.79
				5.89	36.08
				1.67	27.12

References

Abrantes, F., 1988. Diatom productivity peak and increased circulation during the latest Quaternary: Alboran Basin (western Mediterranean). Mar. Micropaleontol. 13, 79–96.

Bárcena, M.A., Abrantes, F., 1998. Evidence of a high-productivity area off the coast of Malaga from studies of diatoms in surface sediments. Mar. Micropaleontol. 35, 91–103.

Brand, L.E., 1994. Physiological ecology of marine coccolithophores. In: Winter, A., Siesser, A. (Eds.), Coccolithophores. Cambridge University Press, Cambridge, pp. 39–49.

Castradori, D., 1998. Calcareous nannofossils in the basal Zanclean of the eastern Mediterranean Sea: remarks on paleoceanography and sapropel formation. Proc. Ocean Drill. Program Sci. Results 160, 113–123.

Chepstow-Lusty, A., Backman, J., Shackleton, N.J., 1989. Comparison of Upper Pliocene *Discoaster* abundance variations from North Atlantic Sites 522, 607, 659, 658 and 662: further evidence for marine plankton responding to orbital forcing. Proc. Ocean Drill. Program Sci. Results 108, 121–141.

Chepstow-Lusty, A., Backman, J., Shackleton, N.J., 1992. Comparison of Upper Pliocene *Discoaster* abundance variations from the Atlantic, Pacific and Indian Oceans: the significance of productivity pressure at low latitudes. Mem. Sci. Geol. 44, 357–373.

Colmenero-Hidalgo, E., Flores, J.A., Sierro, F.J., Bárcena, M.A., Lowemark, L., Schönfeld, J., Grimalt, J., 2004. Ocean surface water response to short-term climate changes revealed by coccolithophores from the Gulf of Cadiz (NE Atlantic) and Alboran Sea (W Mediterranean). Palaeogeogr. Palaeoclimatol. Palaeoecol. 205, 317–336.

Comas, M., Zahn, R., Klaus, A., 1996. Proc. Ocean Drill. Program, Initial Results, vol. 161. Ocean Drilling Program, College Station, TX.

Cramp, A., O'Sullivan, G., 1999. Neogene sapropels in the Mediterranean: a review. Mar. Geol. 153, 11–28.

De Kaenel, E., Villa, G., 1996. Oligocene–Miocene calcareous nannofossil biostratigraphy and paleoecology from the Iberia abyssal plain. Proc. Ocean Drill. Program Sci. Results 149, 79–105.

Emeis, K.C., Robertson, A.H.F., Richter, C., 1996. Proc. Ocean Drill. Program, Initial Results, vol. 160. Ocean Drilling Program, College Station, TX.

Fairbanks, R.G., Wiebe, P.H., 1980. Foraminifera and Chlorophyll Maximum: vertical distribution, seasonal succession, and paleoceanographic significance. Science 209, 1524–1526.

Fairbanks, R.G., Sverdlove, M., Free, R., Wiebe, P.M., Bé, A.W.H., 1982. Vertical distribution and isotopic fractionation of living planktonic foraminifera from the Panama Basin. Nature 298, 841–844.

Filippelli, G., 2001. Carbon and phosphorus cycling in anoxic sediments of the Saanich Inlet, British Columbia. Mar. Geol. 174, 307–321.

Filippelli, G.M., Sierro, F.J., Flores, J.A., Vázquez, A., Utrilla, R., Pérez-Folgado, M., Latimer, J.C., 2003. A sediment-nutrient oxygen feedback responsible for productivity variations in Late Miocene sapropel sequences of the Western Mediterranean. Palaeogeogr. Palaeoclimatol. Palaeoecol. 190, 335–348.

Flores, J.A., Sierro, F.J., 1987. Calcareous plankton in the Tortonian–Messinian transition series of the northwestern edge of the Guadalquivir basin. Abhandlungen der Geologischen Bundesanstalt 39, 67–84.

Flores, J.A., Sierro, F.J., 1997. Revised technique for calculation of calcareous nannofossil accumulation rates. Micropalentology 43, 321–324.

Flores, J.A., Sierro, F.J., Glaçon, G., 1992. Calcareous plankton analysis in the pre-evaporitic sediments of the ODP site 654 (Tyrrhenian Sea, Western Mediterranean). Micropaleontology 38 (3), 279–288.

Flores, J.A., Sierro, F.J., Raffi, I., 1995. Evolution of the calcareous nannofossil assemblage as a response to the paleoceanographic changes in the eastern equatorial Pacific Ocean from 4 to 2 Ma (Leg 138, Sites 849 and 852). Proc. Ocean Drill. Program Sci. Results 138, 163–176.

Flores, J.A., Marino, M., Sierro, F.J., Hodell, D.A., Charles, C.D., 2003. Calcareous plankton dissolution pattern and coccolithophore assemblages during the last 600 kyr at ODP Site 1089 (Cape Basin, South Atlantic): paleoceanographic implications. Palaeogeog. Palaeoclimatol. Palaeoecol. 196, 409–426.

Geisen, M., Billard, C., Broerse, A., Cros, L., Probert, I., Young, J., 2002. Life-cycle associations involving pairs of holococcolithophorid species: intraspecific variation or cryptic speciation? Eur. J. Phycol. 37, 531–550.

Geitznauer, K.R., Roche, M.B., McIntyre, A., 1977. Coccolith biogeography from North Atlantic and Pacific surface sediments. In: Ramsay, A.T.S. (Ed.), Oceanic Micropaleontology 2. Academic Press, Nueva York, pp. 973–1008.

Giraudeau, J., 1992. Distribution of Recent nannofossils beneath the Benguela system: southwest African continental margin. Mar. Geol. 108, 219–237.

Haq, B.U., Lohmann, G.P., 1976. Early Cenozoic calcareous nannoplankton biogeography of the Atlantic Ocean. Mar. Micropaleontol. 1, 119–194.

Hemleben, C., Spindler, M., Anderson, O.R., 1989. Modern planktic foraminifera. Springer-Verlag, New York.

Hilgen, F.J., 1991. Astronomical calibration of Gauss to Matuyama sapropels in the Mediterranean and implication for the Geomagnetic Polarity Time Scale. Earth Planet. Sci. Lett. 104, 226–244.

Hilgen, F.J., Krijgsman, W., 1999. Cyclostratigraphy and astrochronology of the Tripoli diatomite formation (pre-evaporite Messinian, Sicily, Italy). Terra Nova 11, 16–22.

Hilgen, F.J., Krijgsman, W., Langereis, C.G., Lourens, L.J., Santerelli, A., Zachariasse, W.J., 1995. Extending the astronomical (polarity) time scale into the Miocene. Earth Planet. Sci. Lett. 136, 495–510.

Hsü, K.J., Ryan, W.B.F., Cita, M.B., 1973. Late Miocene desiccation of the Mediterranean. Nature 242, 240–244.

Kidd, R.B., Cita, M.B., Ryan, W.B.F., 1978. Stratigraphy of eastern Mediterranean sapropel sequences recovered during Leg 42A and their paleoenvironmental significance. Initial Rep. DSDP 42, 421–443.

Kouwenhoven, T.J., Seidenkrantz, M.S., van der Zwaan, G.J., 1999. Deep-water changes: the near-synchronous disappearance of a group of benthic foraminifera from the Late Miocene Mediterranean. Palaeogeogr. Palaeoclimatol. Palaeoecol. 152, 259–281.

Krijgsman, W., Hilgen, F.J., Langereis, C.G., Santerelli, A., Zachariasse, W.J., 1995. Late Miocene magnetostratigraphy, biostratigraphy and cyclostratigraphy in the Mediterranean. Earth Planet. Sci. Lett. 136, 475–494.

Krijgsman, W., Hilgen, F.J., Raffi, I., Sierro, F.J., Wilson, D.S., 1999. Chronology, causes and progression of the Messinian salinity crisis. Nature 400, 652–655.

Krijgsman, W., Hilgen, F.J., Fortuin, A., Sierro, F.J., 2001. Astrochronology for the Messinian Sorbas Basin (SE Spain) and orbital (precessional) forcing for evaporate cyclicity. Sediment. Geol. 140, 43–60.

Krijgsman, W., Leewis, M., Garcés, M, Kouwenhoven, T., Kuiper, K., Sierro, F.J., submitted for publication. Tectonic control for evaporite formation in the eastern Betics (Tortonian, Spain). Sediment. Geol.

Laskar, J., 1990. The chaotic motion of the solar system: a numerical estimate of the size of the chaotic zones. Icarus 88, 266–291.

Lohmann, G.P., Carlson, J.J., 1981. Oceanographic significance of Pacific late Miocene calcareous nannoplankton. Mar. Micropaleontol. 6, 553–579.

Martín, J.M., Braga, J.C., 1994. Messinian events in the Sorbas Basin of Southeastern Spain and the implications of the recent history of the Mediterranean. Sediment. Geol. 90, 257–268.

Molfino, B., McIntyre, A., 1990. Precessional forcing of nutricline dynamics in the Equatorial Atlantic. Science 249, 766–769.

Montenat, C., Ott d'Estevou, P., 1996. Late Neogene basins evolving in the Eastern Betic transcurrent fault zone: an illustrated review. In: Friend, P.F., Dabrio, C.J. (Eds.), Tertiary Basins of Spain, the Stratigraphic Record of Crustal Kinematics. Cambridge University Press, Cambridge, pp. 286–372.

Muller, C., 1985. Late Miocene to recent Mediterranean biostratigraphy and paleoenvironments based on calcareous nannoplankton. In: Stanley, J., Wezel, F.C. (Eds.), Geological Evolution of the Mediterranean Basin. Springer-Verlag, New York, pp. 471–485.

Negri, A., Villa, G., 2000. Calcareous nannofossil biostratigraphy, biochronology and paleoecology at the Tortonian/Messinian boundary of the Faneromeni section (Crete). Palaeogeogr. Palaeoclimatol. Palaeoecol. 156, 195–209.

Negri, A., Giunta, S., 2001. Calcareous nannofossil paleoecology in the sapropel S1 of the eastern Ionian sea: paleoceanographic implications. Palaeogeogr. Palaeoclimatol. Palaeoecol. 169, 101–112.

Negri, A., Capodonti, L., Keller, J., 1999a. Calcareous nannofossils, planktic foraminifers and oxygen isotope in the late Quaternary sapropels of the Ionian Sea. Mar. Geol. 151, 84–89.

Negri, A., Giunta, S., Hilgen, F.J., Krijgsman, W., Vai, G.B., 1999b. Calcareous nannofossil biostratigraphy of the M. del Casino section (northern Apenines, Italy) and paleoceanographic conditions at times of late Miocene sapropel formation. Mar. Micropaleontol. 36, 13–30.

Negri, A., Morigi, C., Giunta, S., 2003. Are productivity and stratification important to sapropel deposition? Microfossil evidence from late Pliocene insolation cycle 180 at Vrica, Calabria. Palaeogeogr. Palaeoclimatol. Palaeoecol. 190, 243–255.

Okada, H., McIntyre, A., 1977. Modern coccolithophores of the Pacific and North Atlantic Oceans. Micropaleontology 23 (1), 1–55.

Okada, H., McIntyre, A., 1979. Seasonal distribution of modern coccolithophorids in the western North Atlantic Ocean. Mar. Biol. 54, 319–328.

Ott d'Estevou, P., 1980. Evolution dynamique du bassin neogène de Sorbas (Cordillères Bétiques orientales, Espagne). Doc. Trav. IGAL 1, 1–264.

Pérez-Folgado, M., Sierro, F.J., Bárcena, M.A., Flores, J.A., Vázquez, A., Utrilla, R., Hilgen, F.J., Krijgsman, W., Filippelli, G.M., 2003. Western versus eastern Mediterranean paleoceanographic response to astronomical forcing: a high-resolution microplankton study of precession-controlled sedimentary cycles during the Messinian. Palaeogeogr. Palaeoclimatol. Palaeoecol. 190, 317–334.

Reynolds, L., Thunell, R.C., 1985. Seasonal succession of planktonic foraminifera in the subpolar North Pacific. J. Foraminiferal Res. 15, 282–301.

Rohling, E.J., 1994. Review and new aspects concerning the formation of eastern Mediterranean sapropels. Mar. Geol. 122, 1–28.

Rohling, E.J., Gieskes, W.W.C., 1989. Late Quaternary changes in Mediterranean Intermediate Water density and formation rate. Paleoceanography 4, 531–545.

Rohling, E.J., Hilgen, F.J., 1991. The eastern Mediterranean climate at times of sapropel formation: a review. Geol. Mijnb. 70, 253–264.

Rossignol-Strick, M., 1985. Mediterranean Quaternary sapropels, an immediate response of the African monsoon to variation of insolation. Palaeogeogr. Palaeoclimatol. Palaeoecol. 49, 237–263.

Roth, P.H., 1994. Distribution of coccoliths in ocean sediments. In: Winter, A., Siesser, W. (Eds.), Coccolithophores. Cambridge University Press, Cambridge, pp. 199–218.

Sautter, L.R., Thunell, R.C., 1989. Seasonal succession of planktonic foraminifera: results from a four-year time-series sediment trap experiment in the northeast Pacific. J. Foraminiferal Res. 19, 253–267.

Schenau, S.J., Antonarkou, A., Hilgen, F.J., Lourens, L.J., Nijenhuis, I.A., Van der Weijden, C.H., Zachariasse, W.J., 1999. Organic-rich layers in the Metochia section (Gavdos, Greece): evidence for a single mechanism of sapropel formation during the past 10 My. Mar. Geol. 153, 117–135.

Sierro, F.J., Flores, J.A., Zamarreño, I., Vázquez, A., Utrilla, R., Francés, G., Hilgen, F.J., Krijgsman, W., 1997. Astronomical cyclicity and sapropels in the pre-evaporitic Messinian of the Sorbas basin (Western Mediterranean). Geogaceta 21, 131–134.

Sierro, F.J., Flores, J.A., Zamarreño, I., Vázquez, A., Utrilla, R., Francés, G., Hilgen, F.J., Krijgsman, W., 1999. Messinian preevaporite sapropels and precession-induced oscillations in Western Mediterranean climate. Mar. Geol. 153, 137–146.

Sierro, F.J., Ledesma, S., Flores, J.A., Torrescusa, S., Martínez del Olmo, W., 2000. Sonic and gamma ray astrochronology: cycle to cycle calibration of Atlantic climatic records to Mediterranean sapropels and astronomical oscillations. Geology 28 (8), 695–698.

Sierro, F.J., Hilgen, F.J., Krijgsman, W., Flores, J.A., 2001. The Abad composite (SE Spain): a Mediterranean and global reference section for the Messinian. Palaeogeogr. Palaeoclimatol. Palaeoecol. 168, 141–169.

Sierro, F.J., Flores, J.A., Bárcena, M.A., Vázquez, A., Utrilla, R., Zamarreño, I., 2003. Orbitally-controlled oscillations in the

planktic communities and cyclical changes in western Mediterranean hydrography during the Messinian. Palaeogeogr. Palaeoclimatol. Palaeoecol. 190, 289–316.

Sprovieri, R., Di Stefano, E., Caruso, A., Bonomo, S., 1996. High resolution stratigraphy in the Messinian Tripoli Formation in Sicily. Palaeopelagos 6, 415–435.

Troelstra, S.R., Van der Poel, H.M., Huisman, C.H.A., Geerlings, L.P.A., Dronkert, H., 1980. Paleoecological changes in the latest Miocene of the Sorbas Basin, S.E. Spain. Geol. Mediterr. 8, 115–126.

Van Couvering, J.A., Berggren, W.A., Drake, R.E., Aguirre, E., Curtis, G.H., 1976. The terminal Miocene event. Mar. Micropaleontol. 1, 263–286.

Vázquez, A., Utrilla, R., Zamarreñño, I., Sierro, F.J., Flores, J.A., Francés, G., 2000. Precession-related sapropels of the Messinian Sorbas Basin (south Spain): paleoenvironmental significance. Palaeogeogr. Palaeoclimaol. Palaeoecol. 158, 353–370.

Völk, H.R., Rondeel, H.E., 1964. Zur gliederung des Jungtertiars in beechen von Vera, Südost Spanien. Geol. Mijnb. 43, 310–315.

Young, J.R., 1994. Functions of coccoliths. In: Winter, A., Siesser, W.G. (Eds.), Coccolithophores. Cambridge University Press, Cambridge, pp. 63–82.

Ziveri, P., Rutten, A., de Lange, G.J., Thomson, J., Corselli, C., 2000. Present-day coccolith fluxes recorded in central eastern Mediterranean sediment traps and surface sediments. Palaeogeogr. Palaeoclimatol. Palaeoecol. 158, 175–195.